AD-A103 281 MINNESOTA UNIV MINNEAPOLIS DEPT OF AEROSPACE ENGINE--ETC F/G 13/13
STRUCTURAL INELASTICITY XXVII.(U)
APR 81 P G HODGE N00014-75-C-0177
UNCLASSIFIED AEM-H1-27 NL

END
DATE
FILMED
0 81
DTIC

LEVEL II

12

14

Report AEM-H1-27

12 50

AD A103281

6

STRUCTURAL INELASTICITY XXVII

Computer Methods in Plastic Structural Analysis.

10 Philip G. Hodge, Jr., Professor of Mechanics
~~James Malone~~, Research Assistant

Department of Aerospace Engineering and Mechanics
University of Minnesota
Minneapolis, Minnesota 55455

9 Technical rept.,

DTIC
ELECTE
AUG 25 1981
S D
H

15 N00014-75-C-0177

11 Apr[illegible] [illegible]81

Technical Report

Qualified requesters may obtain copies of this report from DDC.

Prepared for:

OFFICE OF NAVAL RESEARCH
Arlington, VA 22217

OFFICE OF NAVAL RESEARCH
Chicago Branch Office
536 South Clark St.
Chicago, IL 60605

DISTRIBUTION STATEMENT A
Approved for public release;
Distribution Unlimited

81 7 28 040

405395

SECURITY CLASSIFICATION OF THIS PAGE (When Data Entered)

REPORT DOCUMENTATION PAGE		READ INSTRUCTIONS BEFORE COMPLETING FORM
1. REPORT NUMBER AEM-H1-27	2. GOVT ACCESSION NO. AD-A103 281	3. RECIPIENT'S CATALOG NUMBER
4. TITLE (and Subtitle) STRUCTURAL INELASTICITY XXVII Computer Methods in Plastic Structural Analysis		5. TYPE OF REPORT & PERIOD COVERED Technical Report
		6. PERFORMING ORG. REPORT NUMBER
7. AUTHOR(s) Philip G. Hodge, Jr., Professor of Mech. James Malone, Research Assistant		8. CONTRACT OR GRANT NUMBER(s) N14-75-C-0177
9. PERFORMING ORGANIZATION NAME AND ADDRESS University of Minnesota Minneapolis, Minnesota 55455		10. PROGRAM ELEMENT, PROJECT, TASK AREA & WORK UNIT NUMBERS NF 064-429
11. CONTROLLING OFFICE NAME AND ADDRESS OFFICE OF NAVAL RESEARCH Arlington, VA 22217		12. REPORT DATE April 1981
		13. NUMBER OF PAGES 97
14. MONITORING AGENCY NAME & ADDRESS (if different from Controlling Office) OFFICE OF NAVAL RESEARCH Chicago Branch Office 536 South Clark St. Chicago, IL 60605		15. SECURITY CLASS. (of this report) Unclassified
		15a. DECLASSIFICATION/DOWNGRADING SCHEDULE

16. DISTRIBUTION STATEMENT (of this Report)

Qualified requesters may obtain copies of this report from DDC

17. DISTRIBUTION STATEMENT (of the abstract entered in Block 20, if different from Report)

18. SUPPLEMENTARY NOTES

19. KEY WORDS (Continue on reverse side if necessary and identify by block number)

Plasticity, Numerical Methods, Linear Programming, Minimization, SUMT, Finite Elements, Simplex Grids, Plates, Arches.

20. ABSTRACT (Continue on reverse side if necessary and identify by block number)

A tutorial review is presented of some of the computer methods useful in the plastic analysis of structures. Each method is illustrated with a trivially simple problem which can be solved without a computer and by one or more larger problems solved with the aid of a computer. The methods described include direct elastic plastic analysis, linear programming, gradient and simplex methods for unconstrained minimization, the SUMT method for constrained minimization, and use of finite-element methods for plate problems. Applications are made to trusses, frames, grids, arches, and plates.

COMPUTER METHODS IN
PLASTIC STRUCTURAL ANALYSIS[1]

by

Philip G. Hodge, Jr.

and

James Malone

1. The material presented in this report will also appear as Chapter 14 in a revised edition of Ref. [7] to be issued by R. Krieger, Melbourne, FL.

1. Introduction. Various methods are available for solving problems in plastic structural analysis. For example, the method of moment-distribution developed by Horne [1] and English [2], the method of superposition of mechanisms first used by Symonds and Neal [3,4], and the method of inequalities due to Dines [5,6] provide three quite different approaches for finding the yield point load of framed structures [7]. When the problem at hand is relatively simple any of these methods may enable one to obtain solutions either in closed form or with a minimal amount of numerical or graphical work. However when these methods are applied to more complex problems, their application may become prohibitively laborious without the aid of a high-speed digital computer.

Now, these plastic methods are sometimes as much art as science. For example, the moment-distribution method assumes any equilibrated moment distribution for a frame and then attempts to reduce the maximum moments in the frame while still satisfying the equilibrium equations. However, there are no rigid rules as to how the largest moments should be redistributed in order to bring about this reduction. Indeed, the number of steps required to obtain the final solution depends primarily on the level of experience of the person solving the problem.

Similarly, the method of superposition of mechanisms as applied to a rectangular portal frame regards any collapse mechanism as a combination of elementary mechanisms, (Fig. 1) each of which corresponds to one independent equilibrium equation for the frame. The method of superposition of mechanisms is systematic in the sense that one first determines the load corresponding to each

elementary panel and beam mechanism to obtain an upper bound for the collapse load. One then attempts to reduce the upper bound by considering combinations of elementary mechanisms, thereby ultimately arriving at the collapse load. The actual choice of combination relies on the fact that an improved upper bound will be obtained only if some hinges present in the original mechanism are eliminated or at least their rotations reduced. Thus there is considerable ingenuity required in choosing which combination of elementary mechanisms is likely to reduce the upper bound.

However, it is exceedingly difficult to program either "engineering judgement" or ingenuity into a computer. The computer will operate only with precisely formulated rules. For example, for the moment-distribution method the computer could be programmed to systematically redistribute the largest moments. However, it would be difficult to protect against getting into an infinite loop, let alone to carry out the reduction in the most efficient manner. In similar fashion if the computer were to use the method of superposition of mechanisms then it would be necessary to consider all of the possible combined mechanisms.

On the other hand, the Dines method of inequalities is completely systematic and could easily be programmed for a computer. In this method the problem is approached statically by first solving the equilibrium equations in terms of a finite set of redundant moments, and then successively eliminating these redundants from the yield inequalities which express the fact that no moment may numerically exceed the yield moment. This elimination is tedious and an original set of $2n$ inequalities on m redundants will lead to the order of $4(n/2)^{2^{m-1}}$ final inequalities on the load. Thus, only

trivially small problems can be solved by hand and moderately large n and m may tax even a large computer. Actually, even here ingenuity can rather drastically reduce the number of inequalities by recognizing inoperative ones at an early stage.

However, the Dines method is only one approach to a set of linear equalities and inequalities. An alternative approach is the simplex method [8] which is described in Sec. 4, herein. This method is cumbersome to do by hand even for small problems, but it can be quite efficiently adapted for computer use.

As suggested by the preceeding discussion, classical methods of plastic structural analysis such as those presented in [7] are useful for solving relatively small problems by hand and for gaining insight into the nature of plastic behavior. However, when solutions to larger problems are required, it is not only necessary to go to the computer, but to modify or replace the methods of solution used for non-computer solutions.

The present report is concerned with several methods of solution which are particularly well adapted to computer calculations. Although some references are cited, there is no attempt to be either current or complete. Rather, a sampling is presented so that the reader may obtain some idea of the types of methods available and the types of problems which can be solved. Further, we begin the various topics with a brief description of the method and a non-computer example involving a trivially simple problem. Large computer programs, like other potent tools, are tremendously valuable when used properly, but can be disasterous when misapplied; it is hoped that the use of simple examples will help convey a basic understanding of the method which should always precede

entrusting the solution to a computer.

Specifically, Secs. 2 and 3 will describe the direct solution of elastic and elastic-plastic trusses under a prescribed loading history. Section 4 gives a brief description of the simplex method use in linear programming, and Sec. 5 applies this method to arbitrarily loaded grids. Sections 6 and 7 are concerned with applications of the theorems of limit analysis which lead to unconstrained or constrained minimization problems. Finally, Secs. 8 and 9 discuss the application of finite-element methods to the upper- and lower-bound theorems of limit analysis.

2. Direct Solution of Elastic Trusses. A general approach to any structural problem is to express the problem in terms of a finite number of unknown quantities, write down sufficient equations to determine those quantities, and then use a computer to obtain a numerical solution of the equations. At least in theory, this approach can be used to find the complete elastic-plastic solution as a function of space and time for any structure under a prescribed load history. However, in order to keep the discussion simple, we shall illustrate the method in relation to trusses.

By definition, a truss is a model of a real structure with the following idealizations. It is composed entirely of uniform straight bars which are connected at their end points by joints which are perfectly free to rotate. The truss is supported only at the joints, and it is loaded only by concentrated forces applied to the joints. Under these conditions the force in each bar will be uniform and directed along the bar, and there is no moment.

Therefore, the static and kinematic state of the truss under load is fully defined by giving the force in each bar and the displacement of each joint. Trusses may be either two- or three-dimensional; for simplicity of exposition we shall discuss only the two-dimensional case.

Consider a given truss which consists of B bars and J joints. The unknowns of the problem will consist of B bar forces and 2J components of joint displacements. If a joint is supported against motion in one or both directions, the corresponding displacement component will be zero but there will be an unknown reaction in that direction so that there are still a total of B + 2J unknowns to determine.

At each joint the bar forces, applied load (which may be zero), and reactions (if any) must be in equilibrium. Thus, (Fig. 2a) the statics of the truss will be expressed by 2J equilibrium equations of the form

$$\begin{aligned} F' \cos\alpha' + F'' \cos\alpha'' + F''' \cos\alpha''' + \ldots + P\cos\beta &= 0 \\ F' \sin\alpha' + F'' \sin\alpha'' + F''' \sin\alpha''' + \ldots + P\sin\beta &= 0 \end{aligned} \tag{1a}$$

The kinematics of a generic bar are shown in Fig. 1-b. Within the restriction of small displacements the extension δ of the bars may be expressed in terms of the joint displacements by B expressions of the form

$$\delta = (u' - u'')\cos\alpha + (v' - v'')\sin\alpha \tag{1b}$$

However, (1b) merely defines a new quantity δ for each bar, so that we still need B additional equations.

These equations must come from the material behavior of the truss. We first make the reasonable assumptions that the extension is uniformly distributed along the bar, and that the state of stress is uniform and uniaxial. If L and A are the length and area of a generic bar, these assumptions may be written

$$\epsilon = \delta/L \qquad \sigma = F/A \tag{1c}$$

where ϵ and σ are the strain and stress components along the bar, and σ is the only non-zero stress component.

We consider first an elastic truss. Then for a generic bar

$$\sigma = E\epsilon \tag{2a}$$

Therefore, it follows from (1c) that the truss must satisfy B equations of the form

$$F = (AE/L)\ \delta \tag{2b}$$

where δ is defined by (1b). Finally, we substitute (2b) and (1b) in (1a) to obtain 2J linear algebraic equations for the 2J unknown displacement components. After these have been solved, Eqs. (1b) and (2b) provide *explicit formulas* for the B bar forces.

EXAMPLE: <u>Six-Bar Truss</u>. As a trivial example we consider the truss of Fig. 3a. The equilibrium equations (1a) can be written by inspection:

$$\begin{aligned}
F_2 + 0.6\ F_6 &= -P & R_{3x} &= -F_1 - 0.6\ F_5 \\
F_3 + 0.8\ F_6 &= P & R_{3y} &= -F_3 - 0.8\ F_5 \\
F_2 + 0.6\ F_5 &= 0 & R_{4x} &= F_1 + 0.6\ F_6 \\
F_4 + 0.8\ F_5 &= 0 & R_{4y} &= -F_4 - 0.8\ F_6
\end{aligned} \tag{3}$$

The kinematic equations (1b) for the six bars are equally simple:

$$\begin{aligned}
\delta_1 &= u_4 - u_3 = 0 & \delta_2 &= u_2 - u_1 \\
\delta_3 &= v_1 - v_3 = v_1 & \delta_4 &= v_2 - v_4 = v_2 \\
\delta_5 &= 0.6\ u_2 + 0.8\ v_2 & \delta_6 &= -0.6\ u_1 + 0.8\ v_1
\end{aligned} \tag{4}$$

Similarly, taking A and E to be the same for all six bars and reading the lengths in inches from Fig. 3, we obtain the elasticity equations (2b) in the form

$$F_1 = (AE/36)\ \delta_1 = 0 \tag{5a}$$

$$F_2 = (AE/36)\ \delta_2 = (AE/36)(u_2 - u_1) \tag{5b}$$

$$F_3 = (AE/48)\ \delta_3 = (AE/48)\ v_1 \tag{5c}$$

$$F_4 = (AE/48)\ \delta_4 = (AE/48)\ v_2 \tag{5d}$$

$$F_5 = (AE/60)\ \delta_5 = (AE/60)(0.6\ u_2 + 0.8\ v_2) \tag{5e}$$

$$F_6 = (AE/60)\ \delta_6 = (AE/60)(-0.6\ u_1 + 0.8\ v_1) \tag{5f}$$

Finally, substitution of (5) in the first column of (3) leads to

$$\begin{aligned}
1.216\ u_1 - 0.288\ v_1 - u_2 &= 36P/AE \\
-0.288\ u_1 + 1.134\ v_1 &= 36P/AE \\
-u_1 + 1.216\ u_2 + 0.288\ v_2 &= 0 \\
0.288\ u_2 + 1.134\ v_2 &= 0
\end{aligned} \tag{6}$$

It is not difficult to solve (6) by hand or with an elementary pocket calculator. However, prepared computer programs are readily available in which one must merely read in introductory information concerning the size of the problem followed by the coefficients on both sides of (6); the program will solve the equations and output the answer. Regardless of method, the solution of (6) is

$$u_1 = 169P/AE \qquad v_1 = 75P/AE$$
$$u_2 = 147P/AE \qquad v_2 = -37P/AE \tag{7a}$$

Substitution of (7a) back into (5) then provides the bars forces

$$F_1 = 0 \qquad F_4 = 0.780\ P$$
$$F_2 = -0.585\ P \qquad F_5 = 0.975\ P \tag{7b}$$
$$F_3 = 1.553\ P \qquad F_6 = -0.691\ P$$

Finally, the second column of (3) gives the reactions.

In actual practice, total computer programs have been developed which do most of the work of solving elastic truss problems. The engineer does not need to explicitly set up Eqs. (3) - (6) but merely needs to provide the program with the nodal coordinates and information about the bars, supports, and loads. For the present example, let the parameters have the values

$$A = 2\ in^2 \qquad E = 30 \times 10^6\ psi \qquad P = 1000\ lb. \tag{8a}$$

Then the input to the program would include the following information, put in whatever format the particular program required:

4 Nodes 6 Bars

Node 1: x = 0.0 y = 36.0, etc.

Bar 1: Nodes 3,4 A = 2.0 E = 30000, etc. (8b)

$u_3 = 0$ $v_3 = 0$, etc.

$P_{1x} = 1.0$ $P_{1y} = 1.0$, etc.

Notice that we may use any set of consistent units. Here we have chosen to give lengths in inches and forces in 1000 lb units (kilopounds or kips).

After receiving this input, the program will then compute the matrix of coefficients* and the right-hand sides of (6), solve the equations, and output the results shown in the first column of Table 1 (p. 70). The units will be the same as in the input data.

EXAMPLE: Wing Truss. The truss in Fig. 4 might represent the framework of an aeroplane wing tip. For purposes of analysis we regard nodes 5, 9, and 12 as fixed, hence the bars joining them are not stressed and will be ignored (the same reasoning could have been used to delete bar 1 in the earlier example). Four different

---

* The actual computation of this matrix is based directly on the elastic principle of minimum potential energy rather than on Eqs. (3) - (5); the result, of course, is the same.

standard 14S aluminum I-beams were used [9, p. 195]. Young's modulus and the yield stress were the same for all beams [9, p. 1372]:

$$E = 10 \times 10^6 \text{ psi} \qquad \sigma_0 = 6 \times 10^3 \text{ psi} \tag{9}$$

The other properties are shown in Table 2. For later approximation by an elastic/perfectly-plastic material σ_0 was taken to be half-way between the 0.2% offset and ultimate yield stresses.

Information analogous to Eqs. (8) was input to the program SAP-4 [10] and was run on the University of Minnesota Cyber 72 computer. Total time in the Central Processor was 1.032 seconds. The results are shown in the "elastic solution" column of Table 3. For this example we chose kips and milli-inches (mils) as the units of force and length, respectively.

3. *Elastic/perfectly-plastic Trusses.* If the bars of a truss are modelled by an elastic/perfectly-plastic material, a complete solution under any prescribed loading history may be obtained by solving a succession of elastic problems and combining the results. The *elastic solution for a unit load* is obtained *first* and the maximum elastic load P_e is found which will just produce the yield force in one bar (or more) and leave all other bars less than yield. If the load is further increased, the bar at yield will continue to transmit its yield force, but the additional load must be carried by the remaining bars. Thus, we now solve a new elastic problem in which a unit load increment is applied to the truss with the *yielding bar* deleted. Denoting the resulting bar forces by $\overline{F}_i$, we can write the total *bar force* F_i *under a load increment* ΔP:

$$F_i = F_{ie} + \Delta P\, \overline{F}_i \tag{10}$$

We then compute ΔP such that one bar in the modified truss is at yield and all other bars are below yield. The process is repeated until sufficient bars have yielded so that when they are removed the remaining truss is a mechanism.

In implementing this procedure it is, of course, necessary to ensure that "*unloading*" *does not occur.* At any stage, the extension increment of a yielded bar can still be computed from Eq. (1b). If $F_i = Y_i$ (the yield force in tension), then the resulting $\Delta\delta_i$ must be positive (or zero); if $F_i = -Y_i$, then $\Delta\delta_i \leq 0$. For most practical situations these requirements will be satisfied, but Refs. [11] and [12] contain relatively simple examples of truss-like structures

where unloading can occur under a single monotonically - increasing external load.

EXAMPLE: Six-Bar Truss. We illustrate the above procedure with the truss of Fig. 3. We take the area and modulus of each bar as in Eq. (8a) and take

$$\sigma_o = 50 \times 10^3 \text{ psi} \tag{11a}$$

as the yield stress for steel. Then, for each bar the yield force is

$$Y = 2 \times 50 \times 10^3 \text{ lb} = 100 \text{ kips} \tag{11b}$$

The general elastic solution is given by Eqs. (7), hence it is clear that bar 3 will yield first (in tension) at a load $P = 64.39$ kips. The resulting complete solution is shown in the column labelled "1L" (Limiting values of stage 1) in Table 1.

Removal of bar 3 from the truss in Fig. 3a leaves the truss in Fig. 3b. Since this truss is statically determinate, one can find the forces directly from statics, Eqs. 1a, and then find the nodal displacements from (2b) and (1b). Alternatively, one may still use the general method described in the preceding section and find the nodal displacements first and then find the bar forces. By either method, the resulting incremental bar forces under a load ΔP are found to be

$$\begin{array}{ll} \Delta F_6 = 1.25\ \Delta P & \Delta F_5 = 2.9167 \Delta P \\ \Delta F_2 = -1.75\ \Delta P & \Delta F_4 = -2.33333 \Delta P \end{array} \tag{12a}$$

and the incremental nodal displacements are

$$\begin{array}{ll} \Delta u_1 = 504\ \ \Delta P/Ae & \Delta v_1 = 471.75\ \Delta P/AE \\ \Delta u_2 = 441\ \ \Delta P/AE & \Delta v_2 = -112\ \Delta P/AE \end{array} \tag{12b}$$

Equations (10) and (12) together with column 1L of Table 1 now show that bar 5 will yield next (in tension) at a load increment defined by

$$F_5 = 62.80 + 2.9167\ \Delta P = 100 \tag{13}$$

Substitution of $\Delta P = 12.75$ into Eqs.(12) gives the incremental solution for stage 2 shown in column 2Δ of Table 1, and addition of these numbers to column 1L gives the total values at the end of stage 2 as shown in column 2L .

During stage 2 the incremental extension of the plastic bar can be found from Eq. (1b) and the computed displacements of node 1:

$$\Delta\delta_3 = \Delta v_1 = 471.75\ \Delta P/AE \tag{14}$$

This value is clearly positive which is consistent with bar 3 yielding in tension. Notice that we may not use Eq. (2b) since bar 3 is no longer elastic.

Removal of bar 5 from the truss of Fig. 3b would produce Fig. 3c which is clearly a mechanism. A formal attempt to solve the defining equations would show that the incremental load ΔP and bar forces ΔF_i would all have to be identically zero, and that the displacements would be indeterminate but could be written

$$\Delta u_1 = \Delta u_2 = 4\Delta\theta \qquad \Delta v_1 = 3\Delta\theta \qquad \Delta v_2 = 0 \tag{15}$$

thus verifying that we have, in fact, reached the collapse load.

The above procedure can easily be computerized. If a program is available for solving elastic trusses, this program can be used to find the incremental solution for each stage for a unit load. This program will print out numbers analogous to those in Eqs. (12) for stage 2. One can then test each bar in Eq. (10) to find the smallest positive ΔP which will produce yielding in tension or compression, multiply the unit incremental solution by this ΔP (column 2Δ in Table 1) and add it to the previous limit solution to find the new limit solution. For a small truss such as the one in Fig. 3, this sequence of steps is easily done with a pocket calculator; for larger trusses this process, too, can be automated. In any event, one then modifies the truss by removing the yielded bar, calls on the elastic truss program to solve the new problem, and repeats the sequence of steps until the collapse load is reached.

EXAMPLE: Wing Truss. The procedure outlined above was used to find the complete elastic-plastic history of the wing truss in Fig. 4, using an interactive computer terminal. A simple program was written which would call on SAP-4 [10] to solve a given elastic truss under a unit load and output the results in a file labelled CHANGE. A second file labelled OLD was initially filled with zero's. A short FORTRAN program was written to read in these two files and the yield force for each bar, and test each bar to find the smallest positive ΔP determined from

$$F_i(\text{OLD}) + \Delta P\, F_i(\text{CHANGE}) = \pm Y_i \tag{16}$$

The program then computed a file NEW to give both forces and displacements from equations analogous to (10). The operator listed this file and, if satisfied with the results, took the following actions:

1. Replaced the values in OLD by those from NEW.
2. "Removed" the plastic member from the truss.

In practice this was done by changing the value of Young's modulus from $E = 10 \times 10^6$ psi as given in (9) to $E = 1 \times 10^{-9}$ psi. This method avoided the necessity of renumbering the bars and also had a further advantage to be mentioned later.

3. Called on SAP-4 to recompute CHANGE for the modified truss.
4. Called the FORTRAN program to read the files, compute a new ΔP, and write a corresponding NEW file.
5. Listed NEW and, if satisfied, repeated the above steps until collapse.

The results are shown in Tables 3. Column 1L gives the maximum elastic solution which is limited by bar 9 reaching its yield force in tension. Column 2Δ shows the incremental solution under a load $\Delta P = 1.34$ kips for the truss with bar 9 removed. Column 2L is the sum of columns 1L and 2Δ and gives the total values at the end of stage 2, determined by bar 4 reaching compressive yield. Similar interpretations apply to columns 3Δ and 3L when bar 20 yields in tension and to 4Δ and 4L when bar 25 yields in compression.

At this point it is clear from Fig. 4 that if the truss has all of bars 4, 9, 20, and 25 removed, it will be free to rotate as a rigid body about node 9. Thus column 4L represents the collapse-load solution. However, it will not always be so obvious

that a mechanism has been created, so it is instructive to observe that the computer program encountered no difficulty in computing a stage 5. To the accuracy called for in listing the file NEW, all force entries in column 5Δ of Table 3b were 0.000 and all displacement entries in Table 3a were 0.000 000 0, so that in both parts of the table column 5L was identical with column 4L. Thus the onset of collapse is signalled by a load increment of zero, and there are no changes in any quantities of interest.

To see what is really occuring in the program in stage 5, we listed the contents of file CHANGE with the results shown in column 5U under a "unit" load of 7.00 kips. Comparison with the solution for the original truss in the "elastic" column, shows that the incremental forces are of the same order of magnitude (except for the yielded bars which are about 10^{-4} less) but the displacements are some 10^{12} times those for the complete truss. Indeed, if we were to reduce the unit load by the factor of 10^{-12}, then the displacements in column 5U would be those of a rigid-body rotation of 0.0014 radians about node 9; in other words, the collapse mechanism. *These results are obtained because we did not completely* remove the yielded bars but replaced them by bars of extreme flexibility, so that we still had a structure to analyze rather than a mechanism.

Finally, before accepting the results of Table 3 we must verify that the yielded bars have always deformed in the proper sense. Applying Eq. (1b) to the four bars in question we obtain

$$\delta_9 = -u_{11} \qquad \delta_{20} = (v_8 - u_8)/\sqrt{2}$$
$$\delta_4 = -u_4 \qquad \delta_{25} = -(v_8 + u_8)/\sqrt{2} \tag{17}$$

Columns 2Δ, 3Δ, 4Δ, and 5U of Table 3a then shown that in each stage, whether elastic or plastic, the changes in δ_9 and δ_{20} are *positive and those in* δ_4 and δ_{25} *are negative.* These results are consistent with the facts that bars 9 and 20 yield in tension, and bars 4 and 25 yield in compression. Therefore, Table 3 represents thy complete elastic-plastic solution up to and including the yield-point load.

An alternative approach would have been to write a master program to perform all of the above steps without operator intervention. Indeed, in a engineering office where large numbers of trusses larger than this one were to be analyzed every day, such *as master program would clearly be preferable.* However, there were several reasons for choosing the present approach.

The authors are not experienced programmers, and several trials were necessary before even this relatively simple procedure worked satisfactorily. Since an interactive computer system was readily available, the debugging of the program was not difficult, and the operator interventions in steps 1 - 5 could be carried *out quite efficiently.*

The program SAP-4 was available as a complete and self-contained "black box" in which a single command enabled data to be input and results would then be put out. The approach which was used took full advantage of the nature of SAP-4 and did not require opening it up to recast as a subroutine. Finally, it was a trivial matter to obtain a listing of the file CHANGE in stage 5 where it was useful without wasting time and paper by listing the earlier stages.

4. Linear Programming. Limit analysis problems can frequently be cast in a form which is known as Linear Programming. The fundamental linear programming problem is to minimize an objective function which is a given linear scalar function of a finite number of variables x_i, subject to the requirements that each x_i be non-negative, and to a finite number of given linear equations. Thus the problem is to minimize

$$\phi = \sum_{j=1}^{n} c_j x_j \tag{18a}$$

subject to

$$x_j \geq 0 \qquad j = 1,\ldots,n \tag{18b}$$

and to

$$\sum_{j=1}^{n} a_{ij} x_j = b_i \qquad i = 1,\ldots,m \tag{18c}$$

where a_{ij}, b_i, and c_j are all given constants, with $b_i \geq 0$. The number of constraints (18c) must be less than the number of variables x_i, $m < n$.

Before relating Eqs. (18) to a limit analysis problem, we formulate the extended linear programming problem in which the variables may also be subject to linear inequalities:

$$\sum_{j=1}^{n} a'_{ij} x_j \leq b'_i \qquad i = 1,\ldots,m' \tag{19a}$$

$$\sum_{j=1}^{n} a''_{ij} x_j \geq b''_i \qquad i = 1,\ldots,m'' \tag{19b}$$

Here b'_i and b''_i are all equal or greater than zero, but there is no restriction on the number of inequalities.

The extended problem can be recast as a fundamental problem by the introduction of "slack variables". Corresponding to each Inequality (19) we write an equation

$$\sum_{j=1}^{n} a'_{ij} x_j + x'_i = b'_i \tag{20a}$$

$$\sum_{j=1}^{n} a''_{ij} x_j - x''_i = b''_i \tag{20b}$$

where the new variables x'_i and x''_i are subject only to

$$x'_i \geq 0 \qquad x''_i \geq 0 \tag{20c}$$

Clearly the restrictions on the original variables x_i embodied in (19) are exactly the same as those in (20). Further, if we replace n and m by $n + m' + m''$ and $m + m' + m''$, respectively, with obvious additions to the a_{ij} and c_j arrays, we can write the extended problem of (18) and (20) in the form of the fundamental problem (18) alone, using the new larger values for n and m.

Now, a typical limit analysis problem involving bending of a beam or frame structure under a given load distribution may be formulated as follows: determine a set of moments M_i which will maximize the load factor f subject to equilibrium equations and upper and lower yield inequalities on the moments. If this problem is to be analogous to the linear programming problem, the moments will correspond to the variables x_i, the equilibrium equations to (18c),

and the yield inequalities to (19a,b). Further, if we define $\phi = -f$, then maximizing f is equivalent to minimizing ϕ. However, since moments may be either positive or negative, we do not appear to have any correspondence to (18b).

This difficulty is easily overcome. Since each moment is subject to a lower yield restriction

$$M_i \geq -M_{i0} \tag{21}$$

we define the linear programming variables by

$$x_i = M_i/M_{i0} + 1 \tag{22}$$

Not only does this substitution correspond to (18b), but it automatically satisfies (19b). Therefore (19) will reduce to

$$x_i \leq 2 \qquad i = 1,\ldots,n \tag{23}$$

and the reduction to the fundamental problem will become particularly simple.

A linear programming problem may have no solution, a solution for which the objective function ϕ is unbounded from below, or a solution with a unique finite value for ϕ. If we start with a real structure (not a mechanism), then the limit analysis problem always has a unique collapse load, so we need consider only the third possibility. However, although ϕ is unique, the values of x_i need not be. If the x_i are unique, then it can be proved [8] that at most m of them are positive and the remaining $n - m$ or more are zero. Here n is the total number of variables including slack variables, and m is the total number of equality constraints (18c) and (20a,b). Even if the x_i are not unique, there will exist at least one

solution at the minimum ϕ for which this statement is true.

Suppose that we can find some set of x_i with $n - m$ of them equal to zero and the rest, called a basis, equal to or greater than zero. Such a set is called a basic feasible solution, and the value of ϕ determined by (18a) is, of course, an upper bound on the minimum ϕ. It is then possible to search all of the non-basic variables and determine if we can reduce the upper bound on ϕ by including any of them in the basis. Further, we can always remove one of the former basic variables in such a way that the new basis will continue to satisfy (18b). Finally, it can be shown that after a finite number of steps (usually between m and 2m [8, p. 52]) this procedure will lead to the minimum ϕ. We shall illustrate the method with a simple example.

EXAMPLE: <u>Simple Frame</u>. We use Fig. 5a to illustrate the formulation and solution of a linear programming problem. The left-hand column is built-in. The right-hand column is pin supported in a fixed location, and hence can support vertical and horizontal reactions, but no moment.

Since only concentrated loads are applied, the moments will be linear between each pair of numbered points and will vanish at 5. Therefore the maximum and minimum values of the moment will occur at the points 1, 2, 3, or 4. There are three possible combinations of yield hinges which can turn the frame into a mechanism, as shown in Fig. 5b-d.

Application of the principle of virtual work to the mechanisms in Fig. 5b and 5c leads to the equilibrium equations

$$-M_2 + 2M_3 - M_4 = 2PL \tag{24a}$$

$$-M_1 + M_2 - M_4 = 6FL \tag{24b}$$

Since Fig. 5d can be regarded as a linear combination of 5b and 5c, the corresponding equilibrium equations will not contain any new information but will be a similar combination of (24a) and (24b). Actually, we find it convenient to replace (24b) by a linear combination with (24a) which will not contain the load. Thus:

$$-M_2 + 2M_3 - M_4 = 2FL \tag{25a}$$

$$M_1 - 4M_2 + 6M_3 - 2M_4 = 0 \tag{25b}$$

Further, we shall use (25a) to define the objective function ϕ, thus leaving (25b) as the single constraint. Making the substitution (22), we obtain

$$\phi \equiv -2FL/M_0 = x_2 - 2x_3 + x_4 \tag{26a}$$

$$x_1 - 4x_2 + 6x_3 - 2x_4 = 1 \tag{26b}$$

Next we introduce four slack variables and replace the inequalities (23) by

$$\begin{aligned} x_1 + x_5 &= 2 \qquad & x_3 + x_7 &= 2 \\ x_2 + x_6 &= 2 \qquad & x_4 + x_8 &= 2 \end{aligned} \tag{26c}$$

The linear programming problem, then is to minimize ϕ defined by (26a), subject to (26b), (26c), and (18b) with $n = 8$.

The solution of this problem is conveniently carried out in a sequence of "Tableaux", as displayed in Table 4. The very top line of the table, labelled "ϕ" lists the coefficients in (26a).

The first five lines of the Table proper are labelled Tableau 0, and are simply a restatement of Eqs. (26b,c) in array form.

In Tableau 1, we have replaced line 2 by a linear combination of lines 1 and 2 (line 2 minus 1), and left all other rows unchanged. The resulting 5 x 8 matrix of coefficients in the eight right-most columns contains a 5 x 5 sub-matrix which is the identity matrix. Clearly, then, if we set $x_2 = x_3 = x_4 = 0$, i.e., choose x_1, x_5, x_6, x_7, and x_8 as a basis, then the values of the basic variables are simply the right-hand sides of the equality constraints, i.e., the values recorded in column RHS. Since these values are all positive, we have defined a basic feasible solution and expressed it in a form which may be termed a unit basic feasible solution.

Two observations are in order at this point. First, the linear combination must be such that all right-hand sides are non-negative. For example, if we had attempted to form the initial basis with x_2 instead of x_1, it follows from line 1 of Tableau 0 that the basic solution would include $x_2 = -1/4$ which is not feasible. Second, we are discussing a particularly simple example in that four of the eight columns in Tableau 0 are already in unit form and the other four contain only two non-zero coefficients, so that it is a trivial matter to construct the unit basic feasible solution of Tableau 1. Although a limit analysis problem will, in general, have a relatively simple Tableau 0 as compared with an arbitrary linear programming problem, it may still prove difficult to find an initial unit basic feasible solution by inspection. In this case, one may use a technique of introducing certain "artificial

variables" [8, Chap. 4, Sec. 3]. In any event, it is always possible to obtain a unit basic feasible solution as a starting point, so we will continue the discussion by describing the remaining entries in Tableau 1.

The column labelled "Basis" lists the basic variables in the order determined by the unit sub-matrix. These happen to be in ascending numerical order, but this fact is unimportant. Column c_j selects those coefficients of (18a), i.e., of the very top line of Table 4, which correspond to the current basis. If the non-basic variables are all zero, the current value of ϕ is

$$\phi_1 = \sum_j{}' c_j \, (RHS)_j \tag{27}$$

where $\sum_j{}'$ refers to the sum over the 5 basic variables only. Since all of these c_j are zero, the result 0 is stored in the c_j column of the line labelled "Test".

Now, suppose that one of the non-basic variables were assigned a unit value while the rest were maintained at zero. In order to continue to satisfy the equality constraints we would have to change the values of the basic variables. These changes may be read directly from Tableau 1 by moving the coefficients in the corresponding column to the other side of the equation. Thus, if we have set the non-basic variable $x_k = 1$, the change in a basic variable x_j will be $-a_{jk}$ where a_{jk} is the coefficient in line j, column x_k of Tableau 1. The change in the objective function caused by these changes in the basic variables will be a <u>de</u>crease of

$$\Delta_k' = \sum_j{}' c_j \, a_{jk} \tag{28a}$$

However, the objective function will also <u>in</u>crease by an amount

$$\Delta_k'' = c_k \tag{28b}$$

since we have changed the non-basic variable x_k from 0 to 1. Therefore, the net improvement in ϕ will be

$$\Delta_k = \Delta_k' - \Delta_k'' = \sum_j{}' c_j \, a_{jk} - c_k \tag{28c}$$

Although Δ_k is significant only for the non-basic variables, we observe that if x_k is a basic variable, then formal application of (28c) leads to

$$\Delta_k = c_k - c_k = 0 \tag{28d}$$

which provides a partial check against errors. The values of Δ_k are listed on the Test line of Tableau 1.

Now if Δ_k is negative, any positive change in the non-basic variable x_k will increase ϕ and hence lead us further from the desired minimum. Therefore, we consider only those non-basic variables for which $\Delta_k > 0$. In the present case Δ_3 is the only positive Δ_k in Tableau 1, so we have circled that value. If more than one $\Delta_k > 0$, we circle the largest one and pick the corresponding variable x_k to become basic. We must now choose which basic variable to delete from Tableau 1. To this end, we examine all positive a_{jk} and compute the ratios $\theta_j = (RHS)_j / a_{jk}$. For Tableau 1, we obtain

$$\theta_1 = 1/6 \qquad \theta_7 = 2 \tag{29}$$

It can be shown [8, Chap. 3] that if we pick the smallest θ_j (note that all $\theta_j \geq 0$) to remove from the basis, then the new basis so obtained will also be feasible. Thus, to obtain Tableau 2 we will replace x_1 by x_3 in the basis, and we have indicated this change by circling $a_{13} = 6$ in Tableau 1.

In order to obtain a new unit feasible basis, we divide line 1 of Tableau 1 by 6 and record the result as line 1 of Tableau 2, labelling it as the new basic variable x_3. Each remaining line in Tableau 2 is now the corresponding line of Tableau 1 plus or minus a multiple of line 1 chosen to make the new $a_{j3} = 0$.

$$\begin{aligned} L_2' &= L_2 + 6L_1' & \qquad L_3' &= L_3 \\ L_4' &= L_4 - L_1' & \qquad L_5' &= L_5 \end{aligned} \tag{30}$$

where we have denoted the Tableau 2 values by primes. Since $c_3 = -2$ and the other basic c_j are still zero, the Test value of ϕ computed from (27) is reduced to -1/3.

As before, the remaining items in the Test line of Tableau 2 are computed from (28). Again, only one of these is positive, so we choose x_2 as the new basic variable and compute

$$\theta_6 = 2/1 = 2 \qquad \theta_7 = \frac{11}{6}/\frac{2}{3} = 2\frac{3}{4} \tag{31}$$

Since θ_6 is the smaller, we replace x_6 by x_2 in the basis and hence obtain the Tableau 3.

The Test value of ϕ has decreased to -1, and all of the Δ_k are now ≤ 0. Therefore any further change in the basis would raise ϕ and Tableau 3 represents the desired *minimum* solution:

$$x_1 = 0 \qquad x_2 = 2 \qquad x_3 = 1.5 \qquad x_4 = 0 \tag{32a}$$

$$x_5 = 2 \qquad x_6 = 0 \qquad x_7 = 0.5 \qquad x_8 = 2 \tag{32b}$$

$$\phi = -1 \tag{32c}$$

Finally substitution of (32) in (22) and (26a), respectively, shows that, with $m_i = M_i/M_0$ and $f = FL/M_0$

$$m_1 = -1 \qquad m_2 = 1 \qquad m_3 = 0.5 \qquad m_4 = -1 \qquad f = 0.5 \tag{33}$$

Clearly the three yield moments correspond to the yield hinges in Fig. 5c and f = 1/2 is the yield-point load for that figure.

5. Grids. In this section we consider problems involving transversely loaded rectangular grids. When the grid is subjected to equal loads at every joint the resulting deformation patterns are reasonably simple and it is a relatively straightforward matter to apply the principle of virtual work and so obtain an upper bound. Further it is not difficult to construct a statically admissible moment distribution for the best upper bound in order to verify that the true collapse load has, in fact, been found.

However, the situation may be quite different if only part of the grid is loaded. In this case, it may be difficult to predict a deformation pattern which will result in an improved

upper bound for the collapse load. Moreover, this deformation pattern may not have an associated statically admissible moment distribution. These problems are illustrated by considering the example of a square grid with a single *load applied* to the intersection nearest a corner, Fig. 6a. We shall assume for simplicity that all four *edges* of the grid are either clamped or simply supported.

We first consider the local deformation pattern shown in Fig. 6a. In this figure we show the *clamped grid and denote* positive and negative yield hinges by circles and squares, respectively. The virtual work *equation* is

$$FL\theta = (4 + 4)\ M_o\theta \qquad f \equiv FL/M_o = 8.00 \qquad (34)$$

for any size grid. *Further, it is not difficult* to construct a statically admissible moment field of the type indicated in *Fig. 7.*

If the grid is simply supported, then the ends at B may rotate freely without a hinge so that the work *equation becomes*

$$FL\theta = 2(2 + 1)\ M_o\theta \qquad f^+ = 6.00 \qquad (35a)$$

However, in this case Fig. 7 is no longer admissible and, in fact, there is no *statically* admissible solution associated with Fig. 6a for the simply-supported grid. Thus we must look for a different pattern for the collapse load.

If the grid is larger than three-square *we may consider* the deformation pattern in Fig. 6b. The work equation in this case is

$$FL\theta = 2\left(\frac{2+1}{2} \times \frac{2+1}{2} + \frac{2+1}{4}\right) M_o\theta \qquad f^+ = 6.00 \qquad (35b)$$

Since this is the same value as in Fig. 6a, we still have only an upper bound.

Spreading the pattern further gives poorer bounds. Figure 6c, valid for grids which *are 5-square or larger* has a work equation

$$FL\theta = 2\left(\frac{3+2+1}{3} \times \frac{3+1}{3} + \frac{3+2+1}{9}\right) M_o\theta \qquad f^+ = 6.67 \qquad (35c)$$

and a similar pattern encompassing 5 squares each way leads to

$$FL\theta = 2\left(\frac{4+3+2+1}{4} \times \frac{4+1}{4} + \frac{4+3+2+1}{16}\right) M_o\theta \qquad f^+ = 7.5 \qquad (35d)$$

Clearly we *are* getting *further from* the collapse load with this approach.

Each of Figs. 6 is valid as drawn only for a grid at least one square larger than the deformation pattern. However, for a simply-supported grid of exactly the same size as the deformation pattern, the beam *ends showing negative* hinges will be at the edge and hence free to rotate without yield hinges. Therefore, the external work remains the same but the internal work is reduced by *eliminating* the second *group of* terms in each equation. Thus, instead of Eqs. 35 (a-d), respectively, we obtain the following results.

Two-square grid:

$$FL\theta = 2(2)\ M_o\theta \qquad f^+ = 4 \qquad (36a)$$

Three-square grid:

$$FL\theta = 2(9/4)\ M_o\theta \qquad f^+ = 4.5 \qquad (36b)$$

Four-square grid:

$$FL\theta = 2(24/9)\ M_o\theta \qquad f^+ = 5.33 \tag{36c}$$

Five-square grid:

$$FL\theta = 2(50/16)\ M_o\theta \qquad f^+ = 6.25 \tag{36d}$$

For two-, three-, and four-square grids we have obtained improved upper bounds. Further, it is not difficult to construct statically admissible moment fields and hence verify that Eqs. (36) give the actual collapse loads. However, for the five-square grid the best upper bound is still 6.00, and the true collapse load is still unknown. The reader is challenged to construct a deformation field which produces a lower value of f^+ without looking ahead to Fig. 9b; the authors admit they were unable to anticipate the true pattern.

Although this problem is, at the least, difficult to solve with an upper-bound approach, it adapts itself readily to a lower-bound approach using Linear Programming as described in the previous section. To be specific, we will discuss the five-square grid, although the method is quite general.

Figure 8a shows a diagram of the grid where we have taken advantage of symmetry about one diagonal. The numbers at the beam ends define the unknown moments; e.g. on span AB the moments are M_1 and M_2. All moments are positive when they produce compression on the top.

Figure 8b gives a detail of a generic joint C. Since no loads are applied to the spans, the shear forces at the ends must be equal and opposite. Moment equilibrium of the spans shows that $V_1 = (M_2 - M_4)/L$, etc. Since no load is applied at C, the sum of

the shear forces must vanish:

$$\Sigma V_C = (M_2 - 2M_4 + M_7 - 2M_6 + M_9)/L = 0 \tag{37}$$

As described in Sec. 4, we define new variables x_i by Eqs. (22). Substitution in Eq. (37) then leads to

$$-x_2 + 2x_4 + 2x_6 - x_7 - x_9 = 1 \tag{38c}$$

where we have been careful to write the equation so that the right-hand side is positive. Applying similar reasoning to each of the ten independent joints, we obtain

$$f \equiv FL/M_o = 4x_1 - 2x_2 - 2 \tag{38a}$$

$$-x_1 + 2x_2 + 2x_3 - x_4 - x_5 = 1 \tag{38b}$$

$$-x_4 + 2x_7 + 2x_{10} - x_{13} = 2 \tag{38d}$$

$$-2x_3 + 4x_5 - 2x_8 = 0 \tag{38e}$$

$$-x_5 - x_6 + 2x_8 + 2x_9 - x_{11} - x_{12} = 0 \tag{38f}$$

$$-x_8 - x_{10} + 2x_{11} + 2x_{13} - x_{15} = 1 \tag{38g}$$

$$-2x_9 + 4x_{12} - 2x_{14} = 0 \tag{38h}$$

$$-x_{12} - x_{13} + 2x_{14} + 2x_{15} - x_{16} = 1 \tag{38i}$$

$$-2x_{15} + 4x_{16} = 2 \tag{38j}$$

Since the load occurs only in (38a) we define the objective function

$$\phi = -f - 2 = -4x_1 + 2x_2 \tag{39}$$

We have now defined the following linear programming problem:

> Determine the 16 variables x_i so as to maximize ϕ (defined by Eq. (39) subjected to the 9 equality constraints (38 b-j) and the 16 inequality constraints (23).

A manual solution of this problem using the method of Sec. 4 would be extremely laborious, so that a computer was used. Further, since numerous prepared linear programming programs are available, it was unnecessary to write a program following the Tableau method of the previous section. Rather, we simply called the prepared program LPKODE [13] which was available in the University of Minnesota computer library, read in the data embodied in (39), (38 b-j), and (23) in the specific format called for by LPKODE, and used (39) and (22) to interpret the results.

The computed collapse load is $f = 5.7143$ which can be recognized as 40/7. The resulting moments are shown in Fig. 9a in the form of a free-body diagram. Figure 9b identifies those moments which are at yield and shows the associated collapse mechanism. It will be observed that hinges do not form at some sections where the moment is at yield. This observation is closely tied in with the concept of non-uniqueness.

To discuss this question further, we note that after accounting for symmetry there are 5 yield hinges in Fig. 9b. If, using hindsight, we change those 5 inequalities to equalities, we have a total of 14 equations to determine 16 unknowns. Therefore, the solution is not unique, but contains two redundancies. As

mentioned in the previous section, when a solution is not uniquely determined, there will be a solution in which all redundancies correspond to either original or slack variables equal to zero, i.e., to limiting values of inequality constraints, and Linear Programming will find such a solution. Thus, we can anticipate at least two sections without hinges in which the computed moment is at yield.

Starting with yield moments only at those sections with hinges, it is not difficult to manually construct alternative statically admissible solutions. Fig. 9c, for example, shows one in which there are no redundant yield moments.

6. Unconstrained minimization. The two preceding sections have approached limit analysis problems from below by using the lower-bound theorem and Linear Programming. The problems may also be approached from above by using the upper bound theorem, and the result will be a problem in unconstrained minimization. Indeed, if we can write a general expression for the upper bound ϕ in terms of a certain set of parameters x_i, then clearly the best upper bound will be obtained by choosing the x_i to minimize ϕ.

If ϕ is a continuously-differentiable function of x_i, then all relative minima can be found by setting all $\partial\phi/\partial x_i = 0$ and solving the resulting equations for x_i. If this provides more than one solution, one simply evaluates ϕ for all solutions and chooses the smallest value.

However, the limit analysis problem is not that simple. Consider, for example, the simple frame in Fig. 5. The most general collapse mechanism can be expressed as a linear combination of the mechanisms in Figs. 5b and 5c, and the resultant

internal work may be written

$$W_i = \theta_b(-M_2 + 2M_3 - M_4) + \theta_c(-M_1 + M_2 - M_4)$$
$$= - M_1\theta_c + M_2(\theta_c - \theta_b) + 2M_3\theta_b - M_4(\theta_b + \theta_c) \tag{40}$$

Now at each hinge, either the moment has a magnitude M_0 and the same sign as the total rotation, or the total rotation is zero. Therefore, in either case the internal work may be written $M_0|\theta_i|$ so that the total internal work is

$$W_i = M_0(|\theta_c| + |\theta_c - \theta_b| + 2|\theta_b| + |\theta_b + \theta_c|) \tag{41}$$

Since the external work is

$$W_e = 2FL\theta_b + 6FL\theta_c > 0 \tag{42}$$

the general upper bound on the yield-point load may be written

$$\phi \equiv \frac{FL}{M_0} = \frac{|\theta_c| + |\theta_c - \theta_b| + 2|\theta_b| + |\theta_b + \theta_c|}{2\theta_b + 6\theta_c} \tag{43}$$

Because of the absolute value signs, the function ϕ is only piecewise differentiable. Indeed, in that portion of a θ_b, θ_c plane for which the external work is positive, there are five different equations for ϕ as illustrated in Fig. 10, where we have defined

$$\lambda = \theta_b/\theta_c \tag{44}$$

Further, in each domain $d\phi/d\lambda$ does not change sign, so that the derivative never vanishes. It follows that the minimum value of ϕ must occur along the dividing line between two domains. Clearly the minimum is $\phi = 1/2$ for $\theta_b = 0$ in agreement with the results

found at the end of Sec. 4.

Even if the minimum ϕ occurs when the derivatives vanish, the resulting equations may have to be solved numerically. If this is the case, it may very well be more efficient to take a numerical approach directly to the original minimization problem. We will illustrate two possible such approaches with an example.

EXAMPLE: Plate Bending. We consider a square plate of side 2L and thickness 2H. Coordinates axes are chosen so that the positive z - axis is in the direction of the positively applied load, say downward. The x- and y- axes lie in the plane of the plate.

The total internal work D_i for the plate is

$$D_i = \int_A (M_x K_x + M_y K_y + M_{xy} K_{xy} \tag{45}$$

where the moments per unit length are defined by

$$M_x = \int_{-H}^{H} z\sigma_x \, dz, \text{ etc.} \tag{46}$$

the curvature rates of the middle surface of the plate by

$$K_x = - \frac{\partial^2 W}{\partial X^2}, \qquad K_y = - \frac{\partial^2 W}{\partial Y^2}, \qquad \frac{1}{2} K_{xy} = - \frac{\partial^2 W}{\partial X \partial Y} \tag{47}$$

and W is the vertical component of the velocity field for the middle surface.

If P(X,Y) is the load on the plate then the external work D_e is

$$D_e = \int_A PWdA \tag{48}$$

The moment yield condition is

$$M_x^2 - M_x M_y + M_y^2 + 3M_{xy}^2 = M_o^2 \tag{49}$$

where M_o is the maximum plastic moment. The corresponding curvature rates are

$$K_x = \alpha(2M_x - M_y), \quad K_y = \alpha(2M_y - M_x), \quad K_{xy} = 6\alpha M_{xy} \tag{50}$$

where α is an arbitrary non-negative scalar factor. Replacing the curvature rates in (45) by their values from Eqs. (50) and using (49), we may write

$$D_i = 2M_o^2 \int_A \alpha \, dA \tag{51}$$

Again, using Eqs. (50) and (49) in (51) we obtain

$$D_i = \frac{2}{\sqrt{3}} M_o \int_A \left[K_x^2 + K_x K_y + K_y^2 + \left(\frac{K_{xy}}{2}\right)^2\right]^{1/2} dA \tag{52}$$

which together with Eqs. (47) becomes

$$D_i = \frac{2}{\sqrt{3}} M_o \int_A \left[W_{,XX}^2 + W_{,XX} W_{,YY} + W_{,YY}^2 + W_{,XY}^2\right]^{1/2} dA \tag{53}$$

We now define dimensionless quantities

$$x = \frac{X}{L}, \quad y = \frac{Y}{L}$$

$$a = \frac{A}{L^2}, \quad d = \frac{\sqrt{3}\, D}{2M_o H} \tag{54}$$

$$p = \frac{PL^2}{6M_o}, \quad w = \frac{W}{H}$$

It now follows from Eqs. (53) and (48) that

$$d_i = \int_a \left[w_{,xx}^2 + w_{,xx} w_{,yy} + w_{,yy}^2 + (w_{,xy})^2\right]^{1/2} da \tag{55}$$

$$d_e = 3\sqrt{3} \int_a pw da \tag{56}$$

The total work d_c done along a hinge curve of length 1 is

$$d_c = \int_o^{\ell} \sqrt{\theta_x^2 + \theta_y^2}\, d\ell \tag{57}$$

where θ_x and θ_y are the slope discontinuities of the velocity field w in the directions of the coordinate axes and dl is an element of distance along the hinge curve.

We now consider the particular case of a simply supported plate of side 2L subjected to a uniform load p/4 over the shaded part of the plate in Fig. 11a., and free from load on the unshaded part. Because of symmetry, it is sufficient to consider one-eighth of the plate as shown in Fig. 11b. We divide this part into two regions by the straight line OD and assume that the velocity field is linear in region 1 and quadratic in region 2. The most general such field is

$$w_1 = \delta(1 - x) \tag{58a}$$

$$w_2 = \delta(1 - x)[1 - \mu(y - \zeta x)] \tag{58b}$$

where ζ and μ are parameters to be determined, and

$$0 \le \zeta \le 1 \tag{59}$$

The dimensionless external work, Eq. (56) for the entire plate is easily found to be

$$
\begin{aligned}
d_e &= \sqrt{3}p\delta\eta \quad \text{if} \quad \eta < \zeta \\
d_e &= \sqrt{3}p\delta[\eta - \mu(\eta - \zeta)^2/4] \quad \text{if } \eta > \zeta
\end{aligned}
\tag{60}
$$

Internal work will be done in region 2 and along hinge lines OD and OC. The slope is continuous (zero) across OA and no work is done in region 1 since w is linear. Thus, the total dimensionless internal work is

$$d_i = 8d_2 + 8d_{OD} + 4d_{OC} \tag{61}$$

Equation (55) shows that

$$
\begin{aligned}
d_2 &= \int_0^1 \int_{\zeta x}^{x} \delta|\mu|\sqrt{1 + 4\zeta^2}\, dydx \\
&= \frac{1}{2}\delta|\mu|(1-\zeta)\sqrt{1 + 4\zeta^2}
\end{aligned}
\tag{62}
$$

Along OD, $y = \zeta x$ and the slope discontinuities between regions 1 and 2 are

$$\theta_x = \delta\mu\zeta(1 - x) \qquad \theta_y = \delta\mu(1 - x) \tag{63}$$

hence it follows from Eq. (57) that

$$d_{OD} = \frac{1}{2}\delta|\mu|(1 + \zeta^2) \tag{64}$$

Along OC, $y = x$ and the slopes are

$$w_{,x} = \delta[\mu(1 - 2\zeta)x - 1 + \mu\zeta] \qquad w_{,y} = -\delta\mu(1 - x) \tag{65}$$

On the other side of OC, symmetry demands that $w_{,x}$ and $w_{,y}$ be interchanged, hence the discontinuities in slope are

$$\theta_x = -\theta_y = \delta(2\mu\zeta x + 1 - \mu - \mu\zeta) \tag{66}$$

Equation (57) then reduces to

$$d_{OC} = 2\int_0^1 |\theta_x|\, dx \tag{67}$$

where θ_x is given by (66).

For values of ζ satisfying (59) the integral for d_{OC} will have three different forms, depending on whether θ_x is always positive, always negative, or changes from negative to positive as x goes from 0 to 1. It is easily shown that

$$d_{OC} = \delta g(\mu,\zeta) \tag{68}$$

where we have defined

$$
g(\mu,\zeta) = \begin{cases} 2(1-\mu) & \text{if} \quad \mu < 1/(1+\zeta) \\ 2(\mu-1) & \text{if} \quad \mu > 1/(1-\zeta) \\ \mu\zeta + (1-\mu)^2/\mu\zeta & \text{otherwise} \end{cases}
\tag{69a}
$$

Finally, we equate d_i to d_e and introduce the further definitions

$$h(\zeta) = (1-\zeta)\sqrt{1+4\zeta^2} + 1 + \zeta^2 \tag{69b}$$

$$
d(\mu,\zeta) = \begin{cases} \eta \text{ if } \; 0 < \eta < \zeta \\ \eta - \mu(\eta-\zeta)^2/4 \quad \text{if} \quad \zeta < \eta < 1 \end{cases}
\tag{69c}
$$

to obtain the upper bound

$$p = (4/\sqrt{3})[|\mu|h(\zeta) + g(\mu,\zeta)]/d(\mu,\zeta) \tag{70}$$

Equation (70) takes on eight different analytic forms depending on the value of μ relative to 0, $1/(1+\zeta)$, $1/(1-\zeta)$, and whether ζ is greater or less than η. Clearly, then, it is not feasible to find its minimum by setting $\partial p/\partial\mu = \partial p/\partial\zeta = 0$. Therefore, we will describe two different numerical methods and apply them to the particular case $\eta = 0.5$.

Gradient Method. We pick any point (μ_1, ζ_1) and evaluate

$$(\nabla p)_1 = (\partial p/\partial\mu,\ \partial p/\partial\zeta)_1$$

at this point using the appropriate formulas. We then move along the negative gradient by considering points

$$\mu = \mu_1 - s(\partial p/\partial\mu)_1 \qquad \zeta = \zeta_1 - s(\partial p/\partial\zeta)_1 \tag{71}$$

and investigate the resulting function

$$\bar{p}(s) = p[\mu(s),\ \zeta(s)] \tag{72}$$

To this end, we consider a sequence of values s_j where $s_0 = 0$, s_1 is assigned, $s_2 = 2s_1$, and $s_j = s_{j-2} + s_{j-1}$ for $j \geq 3$. We evaluate the sequence $p_j = \bar{p}(s_j)$ until we come to a value $j = \ell+1$ such that $p_{\ell+1} > p_\ell$. If $\ell = 0$, we restart the search with a smaller s_1, say 0.1 times the previous value. Otherwise, the three successive values $p_{\ell-1}$, p_ℓ, $p_{\ell+1}$ will be points on a parabola whose vertex is at

$$s^* = \frac{(s_{\ell+1} + s_\ell)q_{\ell-1} + (s_{\ell+1} + s_{\ell-1})q_\ell + (s_\ell + s_{\ell-1})q_{\ell+1}}{2(q_{\ell-1} + q_\ell + q_{\ell+1})} \tag{73a}$$

where

$$q_{\ell-1} = p_{\ell-1}/(s_{\ell-1} - s_\ell)(s_{\ell-1} - s_{\ell+1})$$

$$q_\ell = p_\ell/(s_\ell - s_{\ell-1})(s_\ell - s_{\ell+1}) \tag{73b}$$

$$q_{\ell+1} = p_{\ell+1}/(s_{\ell+1} - s_\ell)(s_{\ell+1} - s_{\ell-1})$$

Finally, we compute a new starting point (μ_2, ζ_2) by substituting s^* in (71), find the gradient $(\nabla p)_2$ and repeat the search along points defined by

$$\mu = \mu_2 - s(\partial p/\partial\mu)_2$$
$$\zeta = \zeta_2 - s(\partial p/\partial\zeta)_2 \tag{74}$$

and continue the process until the step size and/or decrease in p reaches a prescribed criterion.

Geometrically, the first step s_1 from a point (μ_i, ζ_i) is in *the direction of steepest descent* and hence represents the optimum direction for improvement. At s_1, the gradient will, in general, be in a different direction, so we are no longer optimal. However, it is generally much more time-consuming to compute the gradient than to compute p, so that we continue in the direction $(\nabla p)_1$ until we reach an approximation to the minimum in that direction; then, and only then, do we compute a new gradient.

Figure 12 shows several different paths as determined by different starting points and marked with different arrowheads. Three of the paths converge to a minimum value of $p = 9.02424$ at approximately $\mu = 0.741$, $\zeta = 0.358$, taking from 8 to 13 gradient evaluations, with each linear segment requiring about 5 or 6 function evaluations.

A potential drawback of any numerical *minimization scheme* is that it is difficult to be sure that a global minimum is reached. For example, if the starting point is taken as $\mu = 0.1$, $\zeta = 0.8$, the path will converge to a point on the ζ axis with $\zeta \approx 0.77$ and $p = 9.23760$. For any such point one finds $\partial p/\partial\zeta = 0$. Although $\partial p/\partial\mu$ is not defined at $\mu = 0$, for μ near zero it has the same sign as μ. Therefore, this point represents a local minimum which is rather far from the global minimum in both location and value. For this reason, it is always advisable to test several different starting points before accepting a computed value as a minimum.

Numerous variations may be used. For example, one may take s_ℓ directly to recompute the gradient rather than computing s^*. This was done with the starting point B. It required 17 linear segments to reach p_{min} as opposed to 13 when s^* was used. The difference was primarily in the last steps. Indeed using s^* it took 7 steps to reach $p = 9.02440$ and using s_ℓ it took only 8. This observation is not surprising, since if p is mathematically twice continuously differentiable in a region containing its minimum, it will be increasingly well approximated by a quadratic function in the neighborhood.

Another variation is to terminate a segment when a domain boundary is reached. Indeed, starting point B would represent the end of the first segment from A according to this rule. It ended up saving one segment in this example, and is probably not worth the additional programming it would take.

Simplex Method. A quite different approach to finding the minimum has been suggested by Nelder and Mead [14]. As applied to this example with two parameters, one begins by choosing three starting points and forming a triangle. The upper bound p is evaluated at each vertex, and the vertices are denoted by H, M, and L in order of decreasing values of *p*. The object is to form a new triangle by moving H along the line through H and the point K halfway between M and L in order to find a lower value of p.

There are three basic operations for moving H: "reflection," "expansion," and "contraction," and a further operation of "dimunition" can be used to avoid getting *in an* infinite loop. Figure 13 is a flow chart which shows the order in which operations are tested.

One first tries reflection by moving H to H' an equal distance the other side of K as illustrated in Fig. 14a. The changes from triangles 2 to 3 and from 3 to 4 in Fig. 14a represent reflections.

If $p_H' < p_L$, then one tries an expansion in which H' is moved the same distance again along HK to a new position H". The new triangle is then H'LM or H"LM, depending on whether p_H' or p_H'' is the lower. The new vertices must be relabeled, of course, to recognize the new lowest value of p.

If $p_L < p_H' < p_M$, then the reflected triangle H'LM becomes the new one with no further tests being done.

If $p_M < p_H' < p_H$, H is replaced by H' and a "contraction" is tried in which H is moved (from its new position) to H" halfway back towards K, as shown in Fig. 14b. If $p_H < p_H'$, then a contraction is carried out on the original triangle as in Fig. 14c. If $p_H'' < p_H$, it is accepted and a new triangle is formed.

Finally, if contraction does not provide an improved value of p_H, a "diminution" is performed in which both H (original or

reflected) and M are moved to new positions H* and M* halfway towards L to form a new triangle as shown in Fig. 14d.

In the present example, the only diminution occurs in the first triangle, Fig. 12a. A reflection first produces point C' ($\mu = 1/3$, $\zeta = 1$) with $p_C' = 9.23760$. Since this value is less than p_C but greater than p_A or p_B, C is replaced by C' but testing continues. An expansion is not allowed here, since $\zeta \leq 1$, and a contraction produces $p_C'' = 9.25792$ which is greater than p_C'. Therefore a dimunition is used to obtain triangle 2. Notice that the new $p_H^* = 9.26807$ is greater than p_H'. However, the reflection of D in EF produces a lower value of p whereas if we had kept C' we would be stuck in a loop reflecting between C and C'.

Various steps pictured in Fig. 12c illustrate reflections and contractions. From triangle 12, A is reflected in BC to D, which reduces p to 9.02701. Since this lies between p_B and p_C we immediately take BCD as triangle 13. The reflection of B in DC produces $p_B' = 9.03679$ (not shown). Since this is greater than $p_B = 9.03022$, we instead contract the original triangle to obtain E. Then since $p_E = 9.02719 < p_B$, we take EDC as triangle 14. Next, reflection in CD produces E'. Since $p_E' = 9.02718$ is less than p_E but greater than p_D or p_C, we contract the reflected triangle to get DFC as triangle 15.

Figure 12a, b, c, d shows the history of triangles in ever larger scales as we close in on the minimum. For ease of viewing we have omitted some of the intermediate triangles. With triangle 25 all three vertices have the same value to within six significant figures, and we conclude that p = 9.02424 is the best lower bound obtainable with the present variables.

Including points which were tested but did not become new vertices, i.e. unused expansions or reflections, p was evaluated 49 times to obtain triangle 25. By way of comparison, the gradient path in Fig. 12 starting at A evaluated p 66 times and its gradient 10 times for a total of 86 function evaluations since the gradient has two components. The path starting at B, which is closer to the minimum, evaluated p 72 times and ∇p 12 times for a total of 96 function evaluations. It is interesting that G, which is furthest from the minimum took only 34 evaluations of p and 7 of ∇p for a total of 48. Clearly, in this example, the simplex method is of comparable if not greater efficiency than the more widely known gradient method.

7. Constrained Minimization. Limit analysis problems can frequently be cast in the form of a *problem* of constrained minimization in which the object is to minimize a function $f(X_1, X_2, \ldots, X_n)$ subject to various constraints on the variables X_i. Indeed, the linear programming problem discussed in the preceeding two sections represents a particular case of a constrained minimization problem in which the objective function f and all the constraints are linear.

The general problem where the *objective function* and constraints may all be nonlinear is complicated by the fact that the minimum may be either in the interior of the domain or on one or more of its boundaries - and quite different techniques are appropriate for finding it in the two cases. One method of overcoming this difficulty is to define a new objective function which incorporates the constraints as "penalty functions." To this end, we consider the following technique which was first suggested by Carrol [15] and later justified and programmed by Fiacco and McCormick under the title SUMT: Sequential Unconstrained Minimization Technique [16, 17].

The given problem is to minimize an objective function $f(\underset{\sim}{X})$ where X_i are subject to a finite number m of inequality constraints

$$g_i(\underset{\sim}{X}) \leq 0 \quad i = 1,2,\ldots,m \tag{75}$$

The interior of the *region defined* by the strict Inequalities (75) is called the "feasible domain;" we assume that it exists.

We introduce a strictly positive parameter ζ, and, for all points $\underset{\sim}{X}$ in the feasible domain, we define a "primal function"

$$P(X,\zeta) = f(X) - \zeta \sum_{k=1}^{m} 1/g_i(X) \tag{76}$$

Now, each term $[-\zeta/g_i(\underset{\sim}{X})]$ has the following properties. For any fixed point $\underset{\sim}{X}_o$ in the feasible domain, the term will have a finite positive value, and it will approach zero as ζ tends to zero. On the other hand, for any fixed value $\zeta = \zeta_0$, the term will approach plus infinity as X approaches the boundary $g_i(\underset{\sim}{X}) = 0$ of the feasible domain. Therefore, the function $p(X, \zeta_0)$ must have a minimum in the interior of the feasible domain, and the value of that minimum will be an upper bound on the desired minimum value of $f(\underset{\sim}{X})$. Further, if ζ_0 is sufficiently small, the upper bound should be a good one.

The SUMT technique operates as follows. For a given value $\zeta = \zeta_1$, the location $X = \underset{\sim}{X}_1$ of the minimum value of $P_1 = P(\underset{\sim}{X}_1, \zeta_1)$ is determined. Notice that this problem is one of unconstrained minimization and can be solved by any of the methods described in Sec. 6. The procedure is then repeated to find $\underset{\sim}{X}_2$ and $P_2 = P(\underset{\sim}{X}_2, \zeta_2)$ for a smaller value $\zeta = \zeta_2$, taking $\underset{\sim}{X}_1$ as the initial point in the search for $\underset{\sim}{X}_2$. This process is repeated for a sequence of values $\zeta = \zeta_k$ tending to zero. If the functions f and g_i satisfy certain conditions of continuity and convexity, then it can be rigorously proved [17] that the sequence of points $\underset{\sim}{X}_k$ approaches the location of the minimum of $f(\underset{\sim}{X})$, and the sequence of values $f_k = f(\underset{\sim}{X}_k)$ approaches the minimum value of $f(\underset{\sim}{X})$. Further, in numerous examples treated in [17] and elsewhere, these statements were found to be valid even if f and g_i did not satisfy all of the requirements in the formal proof.

EXAMPLE: Pinned Arch. We first consider a rectangular beam subjected to combined bending and tension. The beam has width 2B and height 2H. Coordinate axes are chosen such that the z-axis is directed downward and the x-axis lies along the axis of the beam. Now consider an arbitrary beam section and let the loads be increased until the section becomes fully plastic. The neutral axis will now be located at a distance ηH from the x-axis as shown in Fig. 15. The axial force N and moment M for this fully plastic state are given by

$$N = \int_A \sigma dA = 2B\sigma_o\left(-\int_{-H}^{\eta H} dz + \int_{\eta H}^{H} dz\right) = -4BH\sigma_o\eta$$

$$M = \int_A \sigma z dA = 2B\sigma_o\left(-\int_{-H}^{\eta H} z dz + \int_{\eta H}^{H} z dz\right) = 2BH^2\sigma_o(1-\eta^2) \tag{77}$$

It is convenient to define dimensionless variables by

$$n = \frac{N}{N_o}, \qquad m = \frac{M}{M_o} \tag{78}$$

so that *Eqs.* (77) *become*

$$n = -\eta, \qquad m = 1-\eta^2, \qquad 0 \le \eta^2 \le 1 \tag{79a}$$

Equations (79a) hold when compressive stresses occur on the top surface. The case of tensile stresses on the top surface may be obtained by reflection of the stress distribution in the plane z=0, *the resulting equations being*

$$n = \eta, \qquad m = -(1-\eta^2), \qquad 0 \le \eta^2 \le 1 \tag{79b}$$

Figure 16 shows the resulting yield curve. Any point on the *curve ABCD corresponds* to a fully plastic section of the beam, points inside the curve represent stress distributions which are less than fully plastic, and for points outside the curve no distribution of stresses can be found which will not exceed the yield stress.

We now consider the particular case of a semi-circular arch of radius A, pin-supported at either *end and* carrying a vertical load 2F at the center. Because of symmetry, the vertical reaction at each support is F. However the horizontal reaction F_h is redundant. Actually, it is convenient to regard the angle χ between the resultant reaction force and the vertical at the arch support as the redundant unknown.

We define the following *dimensionless* quantities:

$$h = \frac{M_o}{2AN_o} \qquad r = \frac{AR}{M_o} \qquad f = \frac{AF}{M_o} \tag{80}$$

Equilibrium of the free-body diagram in Fig. 17b then shows that

$$n(\phi) = -2hr\sin(\chi+\phi) \tag{81}$$

$$m(\phi) = r[\cos\chi - \sin(\chi+\phi)] \tag{82}$$

$$f = r\cos\chi \tag{83}$$

Equations (81) and (82), which are based only on statics, show that the "stress profile" in an m, n plane is a straight line with slope dm/dn = 1/2h. If we start at the support $\phi = \pi/2$, the stress point is n = -2hf, m=0 (point E in Fig. 16). As ϕ decreases the stress point will move down the line to point F at $\phi = \pi/2 - \chi$

and will then move back up the line through point E to point G for $\phi = 0$. Since it is physically evident that m and n are negative at the vertex,

$$0 < \chi < \pi/4 \quad (84)$$

and point G is still in the second quadrant.

The entire profile must lie between the two parabolic areas defined by (79). Clearly, it is sufficient to require that the top of the line at $\phi = 0$ lie on or below the upper parabola (79a) and that the bottom of the line at $\phi = \pi/2 - \chi$ lie on or above the parabola (79b). Therefore, if we denote

$$g_1(r,\chi) = n^2(0) + m(0)-1$$

$$g_2(r,\chi) = n^2(\pi/2-\chi) - m\ (\pi/2-\chi)-1$$

it follows from (83) that any values of r and χ such that

$$g_1(r,\chi) = 4h^2\ r^2\ \sin^2\ \chi + r(\cos\ \chi - \sin\ \chi)-1 \leq 0 \quad (85a)$$

$$g_2(r,\chi) = 4h^2\ r^2 + r(1-\cos\ \chi)-1 \leq 0 \quad (85b)$$

will be statically admissible and hence will provide a lower bound on the yield load (84). Further, it is evident from the physical meaning of r and χ [see Eq. (84)] that

$$g_3(r,\chi) = -\ r \leq 0 \quad (85c)$$

$$g_4(r,\chi) = -\ \chi \leq 0 \quad (85d)$$

$$g_5(r,\chi) = \chi - \pi/4 \leq 0 \quad (85e)$$

Therefore, we can state the problem of finding the collapse load in the following form

Maximize $f(r,\chi)$ as given
by (83) subject to the
five Inequalities (85).

The heavy lines in Fig. 18 show the boundary of the feasible domain (85) and the light dashed lines show some of the level curves of the objective function (84). Now, it is clear from this figure that the maximum value of f will occur at the point C where

$$g_1(r,\chi) = g_2(r,\chi) = 0 \quad (86)$$

and it is not difficult to solve these nonlinear equations numerically. For the particular case h = 0.01 we obtain the solution

$$r = 4.960 \qquad \chi = 0.643 \qquad f = 3.970 \quad (87)$$

However, our purpose in considering this example is to illustrate the SUMT method. Therefore, we form the primal function

$$P(r,\chi,\zeta) = -\ r\cos\ \chi - \zeta\Sigma_{i=1}^{5}\ 1/g_i(r,\chi) \quad (88)$$

Let the initial value $\zeta_1 = 10$ and take the point S at r=1, $\chi = 0.785$ which is just below the boundary $g_5 = 0$ as the starting point for a search. We shall use the method of steepest descent described in Sec. 6 to minimize $p(r,\chi,\zeta_k)$, although the actual SUMT program presented in [17] uses a more powerful second-order gradient method.

Since ζ, is large and we are close to the boundary $g_5 = 0$, the term $10/(\chi-\pi/4)$ dominates P and the gradient is nearly vertical.

The search method described in Sec. 6 must be slightly modified, since it may produce a point outside of the feasible domain. If this happens on the first step, the step is cancelled and the search restarted with s replaced by s/10. If it happens on any later step, the point is recorded as infeasible and is replaced by a point halfway between the previous point and the infeasible one. Further, from now on new points are produced by moving halfway to the recorded infeasible one.

Following this procedure, we obtain the point T as the approximate position of the minimum value of P along ST. The next step leads to point U which is almost back along ST and indicates that T was probably not a very good approximation to the minimum. A more refined procedure could have produced a better value for T, but, on the other hand, the computations required might have exceeded those necessary to find the new gradient at T.

Starting from U, the changes are several orders of magnitude different. Table 5 summarizes the information. In the next 48 steps the minimum moves only from U to 10 in Fig. 18, and the primal function decreases only from 90.55 to 90.41. Clearly, then, the point 10 is a very good approximation to the minimum value of $P(r,\chi,10)$.

We now set $\zeta=1$ and take point 10 as a starting point for a new unconstrained minimization problem. In 50 steps we move only to point 1. In Fig. 18 the points $\odot$ represent the location of the minimum of $P(r,\chi,\zeta)$ for the attached circled value of ζ. Table 6 lists the accompanying minimum values of P and of the lower bound f.

At point 1 we reduce ζ to 0.1. Figure 18 shows the first 15 steps explicitly and jumps to point 0.1 100 steps later. Apparently, the primal function P has a valley or trough which goes from the vicinity of 1 to 0.1 along a curve roughly parallel to the boundary g_2. The valley has a gentle slope along this curve, but rather steep sides perpendicular to it. As a result, from any point which is not precisely on the valley curve, the gradient will be almost perpendicular to the curve, and the quadratic approximation to the minimum ends up slightly on the opposite wall of the valley. The resulting zigzag motion thus represents a very inefficient progress down the valley. Extrapolation techniques are available which can considerably speed up this process, but they were not used in this demonstration example.

The method was continued with smaller and smaller values of ζ until for $\zeta=10^{-11}$ we essentially reached the limiting point C in Fig. 18. The sequence of minima are shown in Fig. 18 and in Table 6. In interpreting Table 6, recall that each entry in the P column is for a different ζ, so that the sequence of P values has no particular significance. However, it follows from Eqs. (88) and (84) that the difference between (-P) and f represents the influence of the penalty functions, so that as we reach the last several lines in Table 6 we are essentially maximizing the lower bound f as is desired.

14.8 Finite Elements - Upper Bounds. Ever since the finite-element method for two-dimensional elasticity problems was first introduced by Turner et al [18] in 1956 it has been a most powerful tool for the solution of many different types of problems in

continuum mechanics. Entire books have been written on the subject [19, 20], and new research is continually being done on extending and improving the technique. Therefore, in this and the next section we shall make no attempt to be *general*, but shall confine our discussion to the bending of plates and, more specifically, to the determination of the collapse load of plates.

The essence of the finite-element method is as follows. The plate is visualized as being made up of a finite number of discrete elements which have in common a finite number of nodes. Within each element an equilibrium moment field or a displacement field is assumed to have a simple mathematical form determined by a finite number of parameters. These parameters must be chosen so that appropriate continuity conditions are satisfied, but a number of free parameters will remain. An upper or lower bound on the collapse load is then found in terms of the parameters, and, finally, the parameters are chosen so as to minimize or maximize the yield-point load.

To be specific, let us assume that the plate is polygonal and divide it into a finite number m of triangular elements. We designate as the n+1 nodes all vertices of triangles and the mid-points of all triangle sides. We consider here the upper-bound problem, and *we denote the downward velocity of node i by w_i.*

In a generic triangle j, we take w to be a general quadratic expression

$$w = Ax^2 + Bxy + Cy^2 + Dx + Ey + F \tag{89}$$

Since there are six nodes associated with triangle j, the 6

constants A,...,F can be uniquely determined in terms of the 6 nodal displacements w_i of those nodes. For example, if triangle j is the *right* isosceles triangle α shown in Fig. 19, then the constants in (89) are given by

$$\begin{aligned} 2A &= w_1 - 2w_2 + w_3 & 2C &= w_1 - 2w_6 + w_5 \\ 2D &= -3w_1 + 4w_2 - w_3 & 2E &= -3w_1 + 4w_6 - w_5 \\ B &= w_1 - w_2 - w_6 + w_4 & F &= w_1 \end{aligned} \tag{90}$$

The dimensionless internal energy rate over the generic triangle j is obtained by substituting (89) in (55):

$$\dot{d}_{i(j)} = (4A^2 + 4AC + 4C^2 + B^2)^{1/2} a_j \tag{91}$$

where A, B, C can be expressed in terms of the w_i by expressions analogous to (90), and a_j is the area of the triangle.

Now, the method of determining the coefficients in terms of the nodal displacements guarantees that w and hence $\partial w/\partial s$ will be continuous across each element edge. However, $\partial w/\partial n$ will not necessarily be continuous so that each edge is a potential hinge whose energy dissipation rate must be computed from Eq. (57). For example, it follows from (90) for triangle α and similar expressions for triangle β in Fig. 19 that $\dot{\theta}_x = 0$ and

$$\dot{\theta}_y = |\mu||1+\lambda x| \tag{92a}$$

where

$$\mu = -3w_1 + 2w_6 + 2w_9 - (w_5 + w_8)/2 \tag{92b}$$

$$\lambda = (2w_1 - 2w_2 - w_6 - w_9 + w_4 + w_7)/\mu \qquad (92c)$$

Therefore, the energy rate is

$$d_{i(\alpha\beta)} = |\mu| \int_0^2 |1+\lambda x| dx$$

$$= \begin{cases} 2|\mu|(1+\lambda) & \text{if} \quad \lambda \geq -1/2 \\ |\mu|(-2 - 2\lambda - 1/\lambda) & \text{if} \quad \lambda \leq -1/2 \end{cases} \qquad (93)$$

Similar expressions can be obtained for any edge.

The entire polygonal boundary will be made up of a certain subset of element edges, and we assume *that each such element edge* is either free, simply-supported, or clamped along its entire length. If the edge is free, then the node i at its midpoint may have any displacement hence w_i is a *free nodal displacement*. If it is simply-supported or clamped, then w_i must have the value zero. At a vertex node on the edge, w_i will be zero unless both boundary edges meeting at that node *are free*.

If the edge is clamped, then it may be a hinge line with θ equal to the normal derivative along the edge. For example if the vertical edge in triangle α *in* Fig. 19 is part of the clamped edge of the plate, then the internal energy dissipation there will be given by (93) except that now $w_1 = w_6 = w_5 = 0$ and λ and μ are defined by

$$\mu = 2w_2 - w_3/2 \qquad \lambda = (w_4 - w_2)/\mu \qquad (94)$$

instead of by (92 b,c). If the edge is free or simply supported then, of course, there is *no hinge line and* hence *no energy* dissipation.

The total energy dissipation rate is the sum of all the contributions from triangles and edges:

$$d_i = \Sigma_{\text{triangles}} d_{i(j)} + \Sigma_{\text{edges}} d_{i(\alpha\beta)} \qquad (95)$$

Let $\ell(x,y)$ be the given load distribution. Then *the external* energy rate for triangle j is found from (56) and (89):

$$d_{e(j)} = 3\sqrt{3} \int_{a_j} \ell(x,y)(Ax^2 + Bxy + Cy^2 + Dx + Ey + F)da \qquad (96)$$

The constants A,...,F are known in terms of nodal displacements, and there is no complication *due to absolute values.* The total external energy is simply the sum of that over the triangles:

$$d_e = \Sigma_{\text{triangles}} d_{e(j)} \qquad (97)$$

and the upper bound on the load factor p is given by

$$p^+ = d_i/d_e \qquad (98)$$

Clearly, we want to choose the w_i so as to minimize p^+.

Now both the numerator and denominator of (98) are linear *homogeneous functions* of the n+1 nodal displacements w_i so there are really only n degrees of freedom. A general way of *handling* the situation would be to normalize the displacement field by setting

$$d_e = 1 \qquad (99)$$

Equation (99) could either be used as a constraint in which case we have a constrained minimization problem, or it could be

solved for w_{n+1} and the result substituted in (95) and (97) to obtain an unconstrained minimization problem in n variables. However, in most problems there will be at least one vertex node which must obviously undergo a strictly positive displacement at collapse. Let this be node number n+1 and define new variables x_i by

$$x_i = w_i/w_{n+1} \tag{100a}$$

Actually, it turns out that convergence of the numerical minimization is greatly speeded up by using (100a) only at vertex nodes. If i is a midpoint node between vertex nodes j and k, we define

$$x_i = 10(w_i - \frac{w_j + w_k}{2})/w_{n+1} \tag{100b}$$

In any event, substitution of (100) in (98) leaves us with an unconstrained minimization problem for the n variables x_i.

This problem was solved in [21] for numerous plate problems, using the simplex method of minimization described in Sec. 6. Figure 20, taken from [21] shows one quadrant of a simply supported rectangular plate subject to a uniform load. The quadrant was divided into 8 elements. There were 11 boundary nodes with prescribed zero displacement and the problem was normalized with respect to the center displacement w_{14}, so that a function of 13 variables was minimized. Internal energy contributions were made by 8 regions and 11 possible hinge lines. The resulting best upper bound is shown in Fig 21, also taken from [21]. For the particular case of a square plate, the bound represents a slight improvement over 1.155 which is the upper bound associated

with a displacement field in which the plate deforms into a square pyramid [7, Chap. 10].

9. Finite Elements - Lower Bounds. The kinematic approach used in the preceding section is the most usual method used with finite elements. Since the velocity field defined over the finite elements is a kinematically admissible field for the original continuum structure it leads to a true upper bound on the collapse load. Indeed, the basic approach is a quite general one and can be applied to many problems other than plate bending.

A static approach is much more difficult to implement, and it must be individually tailored to the particular problem being considered since various complicating factors are present. We shall illustrate some of these difficulties by considering a polygonal flat plate under piecewise constant transverse loads. For this problem, a family of lower bound finite element solutions can be constructed, and the best member of the family determined by solving a constrained minimization problem.

In order to find a lower bound on the collapse load, we must construct a statically admissible moment field. For a rectangular plate element shown in Fig. 22 vertical equilibrium and moment equilibrium about the x and y axes lead to

$$\frac{\partial S_x}{\partial X} + \frac{\partial S_y}{\partial Y} + P = 0$$

$$\frac{\partial M_x}{\partial X} + \frac{\partial M_{xy}}{\partial Y} - S_x = 0 \qquad (101)$$

$$\frac{\partial M_y}{\partial Y} + \frac{\partial M_{xy}}{\partial X} - S_y = 0$$

Elimination of the shears and introduction of dimensionless quantities

$$m_x = \frac{M_x}{M_o} \quad \text{etc.}$$

$$p = \frac{PA^2}{6M_o} \qquad (102)$$

then leads to the equilibrium equation

$$\frac{\partial^2 m_x}{\partial x^2} + 2\,\frac{\partial^2 m_{xy}}{\partial x \partial y} + \frac{\partial^2 m_y}{\partial y^2} = -\,6p \qquad (103)$$

Any moment field which satisfies (103), the yield inequality

$$m_x^2 - m_x\, m_y + m_y^2 + 3\, m_{xy}^2 \leq 1 \qquad (104)$$

and any boundary conditions on moments may be used to determine a lower bound on the collapse load.

As with the upper bound, we divide the plate into a finite number m of triangular regions. In a generic region j we first define the most general quadratic moment field

$$m_x = A_1x^2 + A_2xy + A_3y^2 + A_4x + A_5y + A_6$$

$$m_y = B_1x^2 + B_2xy + B_3y^2 + B_4x + B_5y + B_6 \qquad (105a)$$

$$m_{xy} = C_1x^2 + C_2xy + C_3y^2 + C_4x + C_5y + C_6$$

Let ℓ_j be the given constant load in region j. Then the limit analysis problem is to find a multiplier p for the entire plate such that the plate just collapses under loads $p\ell_j$. However, we first define a local multiplier by

$$p_j = -(A_1 + B_3 + C_2)/3\ell_j \qquad (105b)$$

Substitution of (105b) in the equilibrium Eq. (103) shows that

$$p_j = p \qquad j = 1,\ldots,m \tag{106}$$

One of Eqs. (106) can be taken as the definition of p, hence there are m-1 constraints (106).

Continuity conditions across an edge between elements are essentially the well-known Kirchoff boundary conditions (see, for example, [22]) which are independent of material behavior. These continuity conditions may be written [21]

$$m_{nn}] = 0 \qquad 2\frac{\partial m_{ns}}{\partial s}] + \frac{\partial m_{nn}}{\partial n}] = 0 \tag{107 a,b}$$

where the symbol] denotes the jump in the quantity preceding, and (107a, b) applies to every internal edge. Further, at each internal vertex, there is an additional condition

$$\Sigma m_{ns}] = 0 \tag{107c}$$

where the twisting moments m_{ns} are taken in a consistently counter-clockwise direction as we proceed around the vertex.

For example, let us consider the two triangles in Fig. 20. We use Eq. (105a) for α and the same expressions with primes for β. Then, along the common edge y = 0 the requirement (107a) leads to

$$B_1x^2 + B_4x + B_6 = B_1'x^2 + B_4'x + B_6' \tag{108}$$

Since this must be true for all values of x_1 we have three constraints:

$$B_1' = B_1 \qquad B_4' = B_4 \qquad B_6' = B_6 \tag{109a}$$

Similarly, Eq. (107b) leads to two more constraints:

$$\begin{aligned} 4C_1' + B_2' &= 4C_1 + B_2 \\ 2C_4' + B_5' &= 2C_4 + C_5 \end{aligned} \tag{109b}$$

Therefore, if there are e internal edges there will be 5e constraints of the type (109a, b).

As an example of (107c), suppose there are two more triangles δ and γ with vertex at 1 in Fig. 19, obtained by reflecting α and β, respectively in line 5-8. Then (107c) would require

$$2(m_{xy}^{\alpha} - m_{xy}^{\beta} + m_{xy}^{\gamma} - m_{xy}^{\delta}) = 0 \tag{110}$$

at point 1. If the coefficients in (105a) for γ and δ are denoted by double and triple primes, respectively, then (110) requires

$$C_6 - C_6' + C_6'' - C_6''' = 0 \tag{111}$$

If there are a total of v internal vertices, there will be v constraints (111).

Along a clamped boundary edge there are no restrictions on the moments, but if there are s simply-supported edges and f free edges there will be 3s + 3f constraints (109a) and 2f constraints (109b) along the boundary. Finally, (111) will provide a constraint at a given vertex only if both the boundary edges meeting at that vertex are free.

As an example, consider the quarter-plate in Fig. 20. There are 8 regions so there are initially 8 x 18 = 144 constants. For this arrangement of elements m = 8, e = 10, v = 3, and s = 5 so that Eqs. (106, 109, 111, and 109a) provide

$$(8 - 1) + 10 \times 5 + 3 + 5 \times 3 = 80 \tag{112a}$$

constraints leaving

$$144 - 80 = 64 \tag{112b}$$

degrees of freedom. Therefore, before proceeding any further we denote 64 of the coefficients as components of a vector $\underset{\sim}{X}$, and we compute and store a matrix $\underset{\sim}{B}$ which expresses all 144 coefficients $\underset{\sim}{A}$ as linear combinations of the 64 components of $\underset{\sim}{X}$:

$$\underset{\sim}{X} = \underset{\sim}{B}\,\underset{\sim}{A} \tag{113}$$

Next, we consider the inequality constraints due to the yield condition. The yield condition (104) is quadratic in the moments, and the moments are linear in X_i and quadratic in x and y. Therefore, we can write the yield constraint as

$$g(X_i, x, y) \leq 0 \tag{114}$$

where g is quadratic in X_i and quartic in x and y. However, the method of constrained minimization cannot handle functional inequalities. Therefore, we pick a finite number k of points x_j, y_j in the plate and require that

$$g_j(X_i) \equiv g(X_i, x_j, y_j) \leq 0 \tag{115}$$

Now, if the points x_j, y_j are fixed, the yield Inequalities (115) will be satisfied at those k points, but may be violated at other points x, y. Indeed, it was found in [21] that it was often grossly violated at some other points. Therefore the solution was not a lower bound as it stood, and if the load were scaled down to satisfy (114) everywhere, the resulting lower bound would be a very poor one.

However, if the k points x_j, y_j include all relative maxima of $g_j(X_i)$, then satisfaction of (115) would clearly guarantee satisfaction of (114) everywhere. Since g_j is fourth power in x and y, the relative maxima must be found numerically. Further, *as the values of X_i change, the very number of relative maxima* may change, thus introducing discontinuities into the primal function P. Therefore, it was found necessary to use both fixed points and relative maxima points in such a way as to keep the total number of constraints constant. As stated in [21], "This process is relatively time-consuming, but it appears to be a necessity for a workable lower bound method".

Once the points x_j, y_j have been chosen, we can formulate the constrained minimization problem as in Sec. 7. A primal function is defined by

$$P(X_i,\zeta) = -p(X_i) - \zeta \sum_{i=1}^{k} 1/g_j(X_i) \tag{116}$$

where $p(X_i)$ is defined by that one of (106) which was not listed as a constraint, along with its associated (105b). The methods of Sec. 7 can be used to minimize P although now, of course, X_i will generally have more than two components.

The method was used for numerous examples in [21]. Figure 21 shows the resulting lower bound for simply-supported rectangular plates under uniform load. Evidently it is reasonably close to the upper bound obtained in the preceding section so that for practical purposes we may regard the collapse load as having been determined. In particular, for a square plate the result is a substantial improvement over the value 0.859 obtained in Ref. 7, Chap. 10.

REFERENCES

1. M. R. Horne: A Moment Distribution Method for the Analysis and Design of Structures by the Plastic Theory, Proc. Inst. Civil Engrs. (London), 3(3), 51-76 (1954).

2. J. M. English: Design of Frames by Relaxation of Yield Hinges, Proc. ASCE, 79 (sep. 322) (1953).

3. B. G. Neal and P. S. Symonds : The Rapid Calculation of the Plastic Collapse Load for a Framed Structure, Proc. Inst. Civil Engrs. (London), 1 (3), 58-71 (1952).

4. P. S. Symonds and B. G. Neal: Recent Progress in the Plastic Methods of Structural Analysis, J. Franklin Inst., 252, 383-407, 469-492 (1951).

5. L. L. Dines: Systems of Linear Inequalities, Ann. Math. Princeton, 20 (2), 191-199 (1918-1919).

6. L. L. Dines: Note on Certain Associated Systems of Linear Equalities and Inequalities, Ann. Math. Princeton, 28 (2) 41-42 (1946).

7. P. G. Hodge, Jr.: "Plastic Analysis of Structures," McGraw-Hill Book Co., New York, 1959.

8. S. I. Gass : "Linear Programming", Second Edition, McGraw-Hill Book Co., New York, 1964.

9. O. W. Eshbach and M. Souders, eds.: "Handbook of Engineering Fundamentals", Third Edition, J. Wiley and Sons, New York, 1975.

10. K. Bathe, E. L. Wilson, and F. E. Peterson, "SAP IV", EERC 73-11, University of California, Berkeley, 1973.

11. D. C. Drucker: Plasticity of Metals - Mathematical Theory and Structural Applications, Trans. Amer. Soc. Civil Engineers, **116**, 1059-1072 (1951).

12. P. G. Hodge, Jr.: Complete Solutions for Elastic-Plastic Trusses, SIAM J. Appl. Math., **25**, 435-447 (1973).

13. T. *Hoffman:* "LPKODE", University of Minnesota Computer Center, 1978.

14. J. A. Nelder and R. Mead: A Simplex Method for Function Minimalization, Computer Journal, **7**, 308-313, (1965).

15. C. W. Carroll: The Created Response Surface Technique for Optimizing Restrained Systems, Operations Research, **9**, 169-184, (1961).

16. G. P. McCormick, W. C. Mylander, and A. V. Fiacco: "Computer Program Implementing the Sequential Unconstrained Minimization Technique for Nonlinear Programing", Research Analysis Corp., McLean, Va. RAC-TP-151 or SHARE Library Program SDA 3189.

17. G. P. McCormick and A. V. Fiacco: "Programming Under Nonlinear Constraints by Unconstrained Minimization: A Primal-Dual Method", Research Analysis Corp., McLean, Va. RAC-TP-96, 1963.

18. M.J. Turner, R. W. Clough, H. C. Martin, and L. J. Topp: Stiffness and Deflection Analysis of Complex Structures, J. Aero Sci., **23**, 805-823, (1956).

19. O. C. Zienkiewicz: "The Finite Element Method in Engineering Science", McGraw-Hill, London, 1971.

20. J. T. Oden: "Finite Elements of Nonlinear Continua", McGraw-Hill Book Co., New York 1972.

21. P. G. Hodge, Jr. and T. Belytschko: Numerical Methods for the Limit Analysis of Plates, J. Appl. Mech., **35**, 796-802, (1968).

22. P. G. Hodge, Jr. "Continuum Mechanics", McGraw-Hill Book Co., New York, 1970.

Table 1

Solution of Six-Bar Truss, Fig. 3

Disp or Force	Elastic	1L	2Δ	2L
u_1	.00209	.181	.107	.288
v_1	.00124	.080	.100	.180
u_2	.00246	.158	.094	.252
v_2	.00062	-.040	-.024	-.064
F_2	-0.585	-37.68	-22.32	-60
F_3	1.553	100	0	100
F_4	0.780	-50.24	-29.76	-80
F_5	0.975	62.80	37.20	100
F_6	-0.691	-44.52	15.94	-26.57
P	1.000	64.39	12.75	77.14

Table 2

Bar Properties of Wing Truss, Fig. 4

Bars	Depth (in)	Web width (in)	Area (in^2)	Yield Force (kips)
5-7 10-13	3.0	0.170	1.67	10.0
21-24 26	4.0	0.190	2.25	13.5
17-19	5.0	0.210	2.92	17.5
all others	6.0	0.230	3.36	22.0

Table 3a

Joint Displacement (Mils) in Truss of Fig. 4 (Load is in Kips)

Displacement	Elastic.	1L	2Δ	2L	3Δ	3L	4Δ	4L	5U
(Load)	7.00	27.92	1.34	29.27	3.52	32.79	0.08	32.86	7.00
u_1	18.3	73	5	78	49	127	2	128	84×10^{12}
v_1	82.6	330	30	359	173	532	7	539	337×10^{12}
u_2	16.7	67	4	71	48	119	2	120	84×10^{12}
v_2	54.0	215	20	235	120	356	5	361	253×10^{12}
u_3	14.1	56	4	60	47	107	2	108	84×10^{12}
v_3	31.7	127	11	138	70	207	3	210	168×10^{12}
u_4	8.4	34	2	36	43	79	1	81	84×10^{12}
v_4	13.6	54	4	58	27	85	1	87	84×10^{12}
u_6	-3.5	-14	-4	-18	-1	-19	-0.3	-19	-.009
v_6	56.2	224	20	244	121	365	5	371	253×10^{12}
u_7	-2.0	-8	-3	-11	-0.1	-11	-0.4	-12	-.007
v_7	31.8	127	12	139	71	209	3	213	168×10^{12}
u_8	0.1	0.4	-1	-0.6	0.3	-0.4	-0.4	-1	-.003
v_8	12.4	49	4	53	19	72	1	73	84×10^{12}
u_{10}	-14.6	-56	-10	-66	-46	-112	-2	-114	-84×10^{12}
v_{10}	38.6	154	13	168	73	240	3	244	168×10^{12}
u_{11}	-9.0	-36	-9	-45	-43	-88	-2	-90	-84×10^{12}
v_{11}	16.4	65	5	71	25	96	1	97	84×10^{12}

Table 3b

Bar Forces (Kips) of Truss in Fig. 4

Bar	Elastic.	1L	2Δ	2L	3Δ	3L	4Δ	4L	5U
(Load)	7.00	27.92	1.34	29.27	3.52	32.79	0.08	32.86	7.00
1	-1.00	-3.99	-0.19	-4.18	-0.50	-4.68	-0.01	-4.69	-0.50
2	-1.60	-6.37	-0.32	-6.69	-0.77	-7.46	-0.01	-7.47	-0.26
3	-3.44	-13.70	-0.94	-14.64	-2.08	-16.72	-0.02	-16.74	0.26
4	-5.15	-20.54	-1.46	-22.00	0	-22.00	0	-22.00	-.001
5	0.41	1.65	0.18	1.83	0.27	2.10	-.007	2.10	0.68
6	0.59	2.36	0.52	2.89	0.11	3.00	-0.02	2.98	1.03
7	-0.03	-0.12	0.30	0.19	-0.07	0.11	0.12	0.23	0.87
8	3.09	12.34	0.39	12.72	1.84	14.56	0.06	14.62	0.77
9	5.52	22.00	0	22.00	0	22.00	0	22.00	.001
10	-0.60	-2.39	-0.12	-2.51	-0.26	-2.77	-.002	-2.78	-1.54
11	-0.02	-0.09	-0.18	-0.27	-0.30	-0.57	0.01	-0.56	-0.51
12	-1.90	-7.57	-0.45	-8.02	-0.64	-8.66	-0.01	-8.67	-2.05
13	0.34	1.37	0.09	1.46	2.26	3.72	0.02	3.74	-1.02
14	-2.47	-9.84	-0.95	-10.79	-3.88	-14.67	-0.11	-14.79	-1.28
15	1.41	5.64	0.27	5.91	0.71	6.62	0.02	6.64	1.02
16	2.11	8.43	0.32	8.76	1.04	9.80	0.03	9.83	-0.26
17	0.85	3.37	0.18	3.55	0.37	3.92	.003	3.93	-0.52
18	2.04	8.15	0.13	8.28	0.73	9.01	0.02	9.03	-0.64
19	1.32	5.25	0.57	5.81	1.14	6.95	.001	6.96	-0.77
20	3.74	14.93	1.46	16.39	5.61	22.00	0	22.00	.001
21	0.97	3.86	0.31	4.17	-3.07	1.10	-0.03	1.07	1.02
22	-1.30	-5.12	-0.31	-5.43	-7.18	-6.15	-0.01	-6.16	-1.02
23	-1.45	-5.80	-0.43	-6.23	-0.13	-6.36	-.001	-6.36	0.13
24	-2.26	-9.01	-0.22	-9.24	-1.55	-10.79	-0.05	-10.85	-0.77
25	-3.81	-15.18	-0.80	-15.99	-5.77	-21.75	-0.25	-22.00	-.001
26	-1.38	-5.52	0.68	-4.84	3.31	-1.51	0.11	-1.40	-0.45

Table 4 Tableaux for Linear Programming

Solution of Frame in Fig. 5

Tableau	Line	Basis	c_j	ϕ	0	1	-2	1	0	0	0	0
				RHS	x_1	x_2	x_3	x_4	x_5	x_6	x_7	x_8
0	1			1	1	-4	6	-2	0	0	0	0
	2			2	1	0	0	0	1	0	0	0
	3			2	0	1	0	0	0	1	0	0
	4			2	0	0	1	0	0	0	1	0
	5			2	0	0	0	1	0	0	0	1
1	1	x_1	0	1	1	-4	6	-2	0	0	0	0
	2	x_5	0	1	0	4	-6	2	1	0	0	0
	3	x_6	0	2	0	1	0	0	0	1	0	0
	4	x_7	0	2	0	0	1	0	0	0	1	0
	5	x_8	0	2	0	0	0	1	0	0	0	1
	Test		0	-	0	-1	2	-1	0	0	0	0
2	1	x_3	-2	1/6	1/6	-2/3	1	-1/3	0	0	0	0
	2	x_5	0	2	1	0	0	0	1	0	0	0
	3	x_6	0	2	0	1	0	0	0	1	0	0
	4	x_7	0	11/6	-1/6	2/3	0	1/3	0	0	1	0
	5	x_8	0	2	0	0	0	1	0	0	0	1
	Test		-1/3	-	-1/3	1/3	0	-1/3	0	0	0	0
3	1	x_2	1	2	0	1	0	0	0	1	0	0
	2	x_3	-2	3/2	1/6	0	1	-1/3	0	2/3	0	0
	3	x_5	0	2	1	0	0	0	1	0	0	0
	4	x_7	0	1/2	-1/6	0	0	1/3	0	-2/3	1	0
	5	x_8	0	2	0	0	0	1	0	0	0	1
	Test		-1	-	-1/3	0	0	-1/3	0	-1/3	0	0

Table 5

Motion of $\underset{\sim}{x}_k$ for $\zeta = 10$

k	Segment	Δr	$\Delta \chi$	ΔP	Δf
1	ST	0	-.538	-25000	.173
2	TU	-.077	.234	-40	-.143
3	-	-.007	.008	-.03	-.009
3-50 (total)	U-10	-.077	-.011	-.14	-.065

Table 6

SUMT method for Pinned Arch

ζ	r	χ	$P(r,\chi,\zeta)$	$f(r,\chi)$	steps
10	.840	.433	90.41	.762	50
1	1.030	.451	8.28	.927	50
.1	3.357	.628	-1.22	2.733	116
.01	3.805	.619	-2.89	3.099	33
.005	4.638	.644	-3.52	3.710	73
.001	4.796	.643	-3.77	3.838	41
10^{-4}	4.884	.643	-3.895	3.908	17
10^{-5}	4.911	.642	-3.929	3.932	55
10^{-6}	4.912	.642	-3.934	3.935	7
10^{-7}	4.913	.642	-3.936	3.936	41
10^{-8}	4.955	.643	-3.965	3.965	10
10^{-9}	4.957	.643	-3.967	3.967	4
10^{-10}	4.958	.643	-3.968	3.968	2
10^{-11}	4.958	.643	-3.969	3.969	11

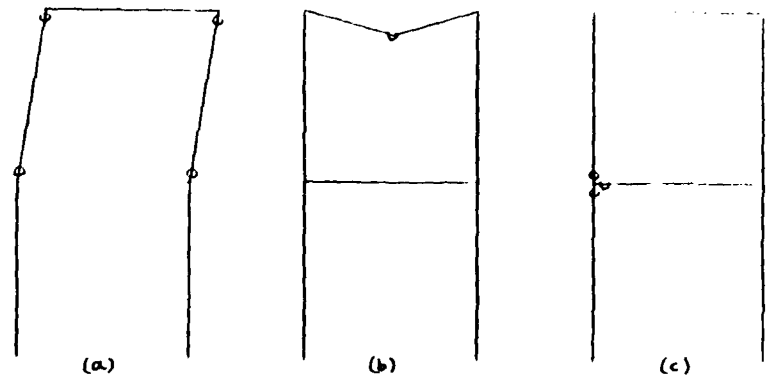

Figure 1: Examples of elementary mechanisms (a) Elementary panel mechanism. (b) Elementary beam mechanism. (c) Elementary joint mechanism.

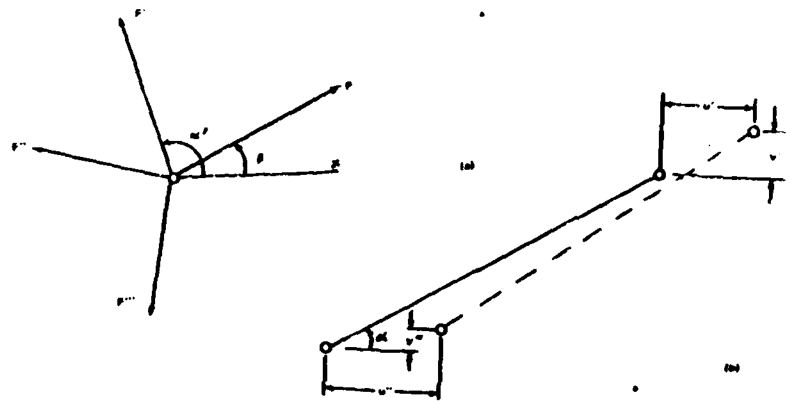

Figure 2: Statics and kinematics of a truss. (a) Statics of a joint. (b) Kinematics of a bar.

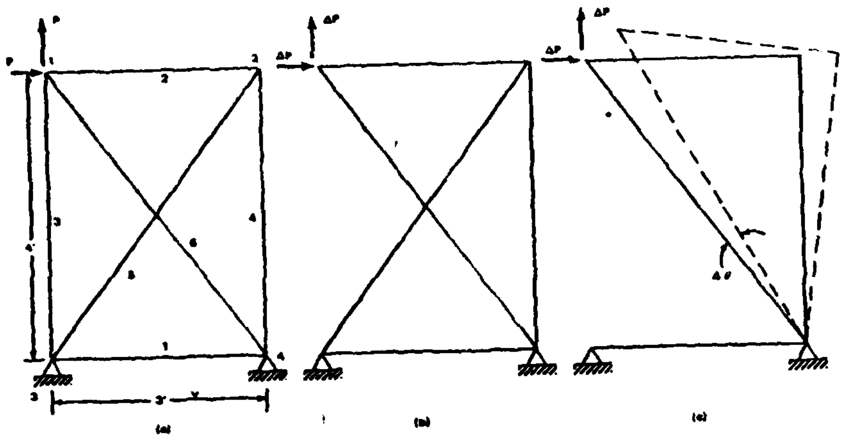

Figure 3: Six-bar truss. (a) Statically-indeterminate truss. (b) Statically-determinate truss with bar 3 removed. (c) Mechanism with bars 3 and 5 removed.

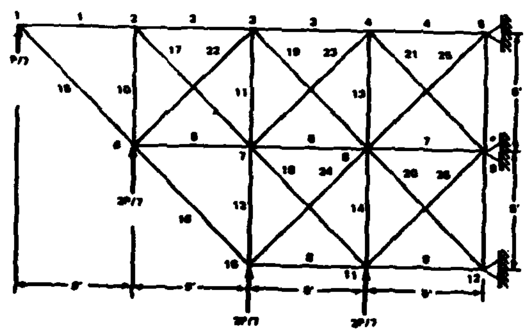

Figure 4: Wing truss.

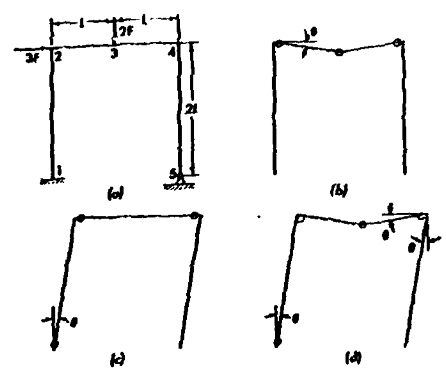

Figure 5: Collapse of simple frame. (a) Loaded frame.
(b) Collapse mode for beam failure only.
(c) Collapse mode for panel failure only.
(d) Combined collapse load.

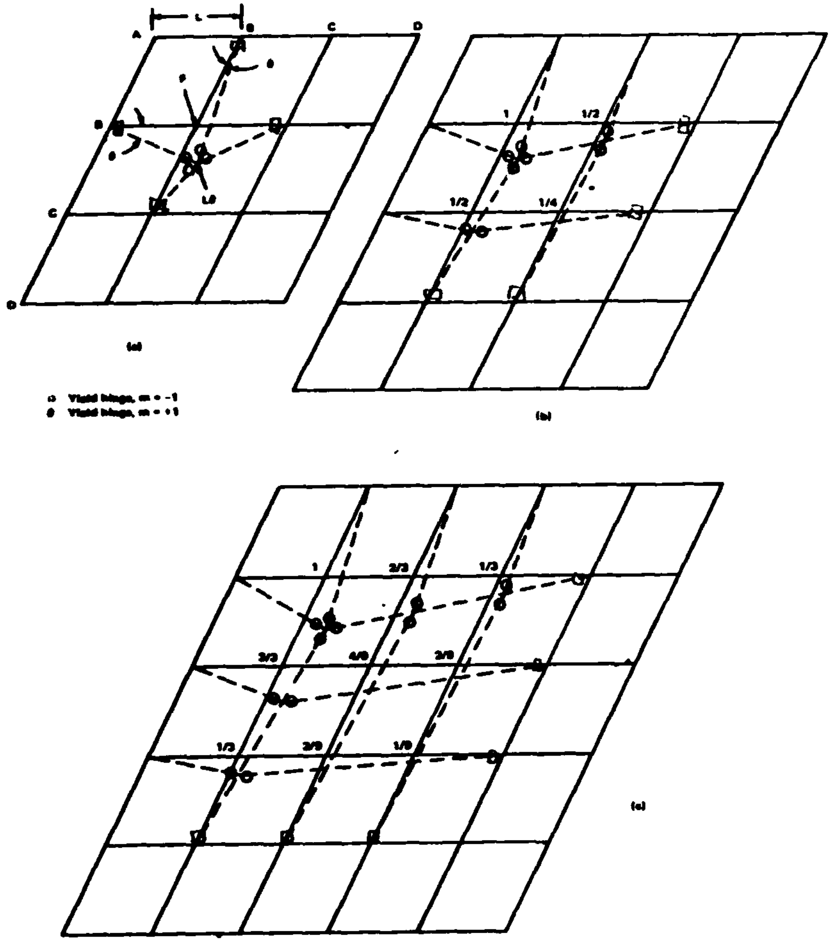

Figure 6: Pyramid deformation grid patterns. (a) $f_{c\ell} = 8.0$, $f_{ss} = 6.0$. (b) $f_{ss} = 6.0$. (c) $f_{ss} = 6.667$.

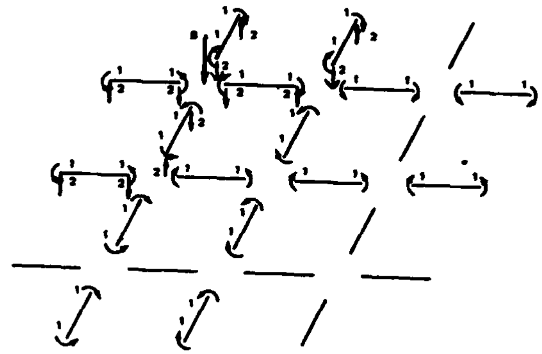

Figure 7: Equilibrium moments and shears for clamped grid in Figure 6. All moments and shears are zero except as shown.

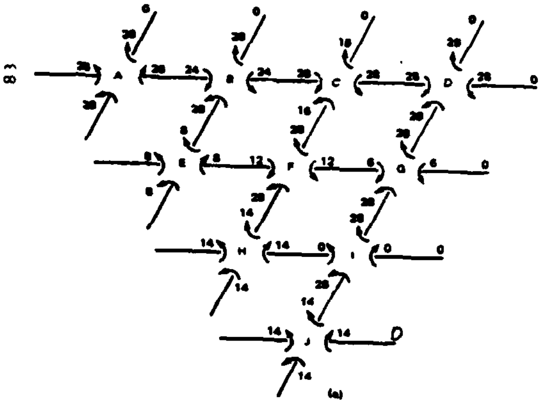

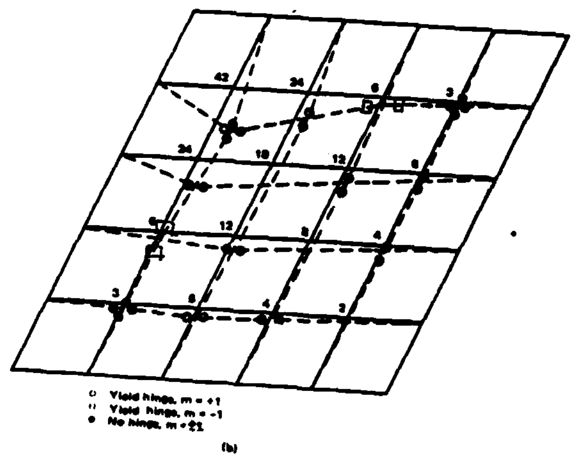

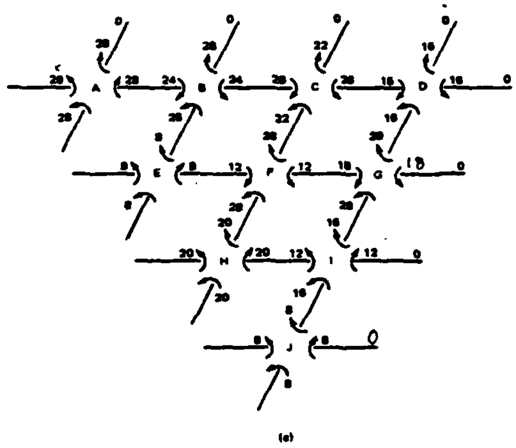

Figure 9: Collapse load solution for 5-square grid under single load. (a) Statically admissible moments given by LPKODE $M_0 = 28$. (b) Deformation pattern. Numbers represent relative displacements of nodes. (c) Alternative statically admissible moments.

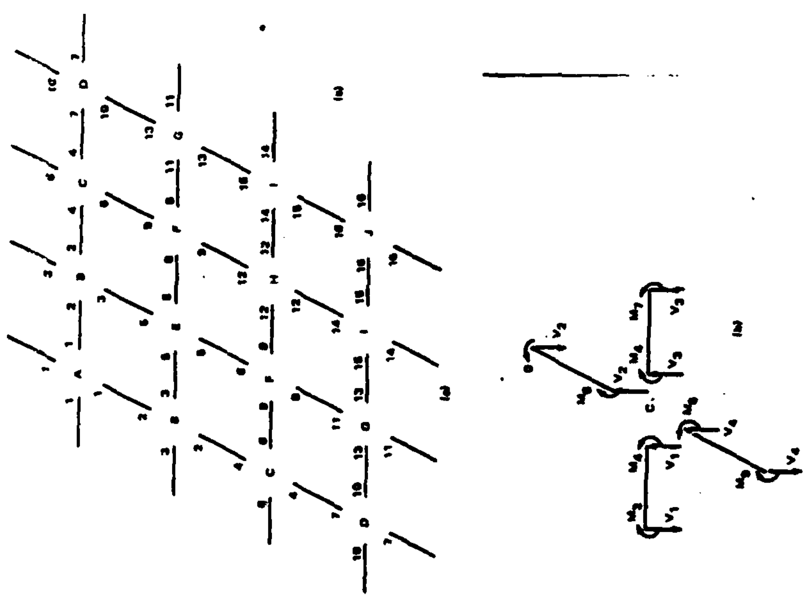

Figure 8: Symmetric moment distribution for 5-square grid. (a) Moment labels. (b) Detail of node C.

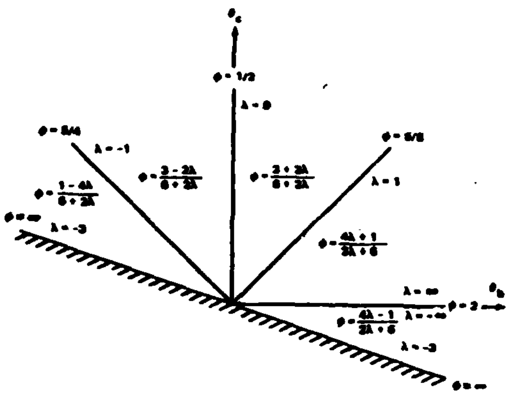

Figure 10: $\theta_b - \theta_c$ plane for frame of Figure 5.

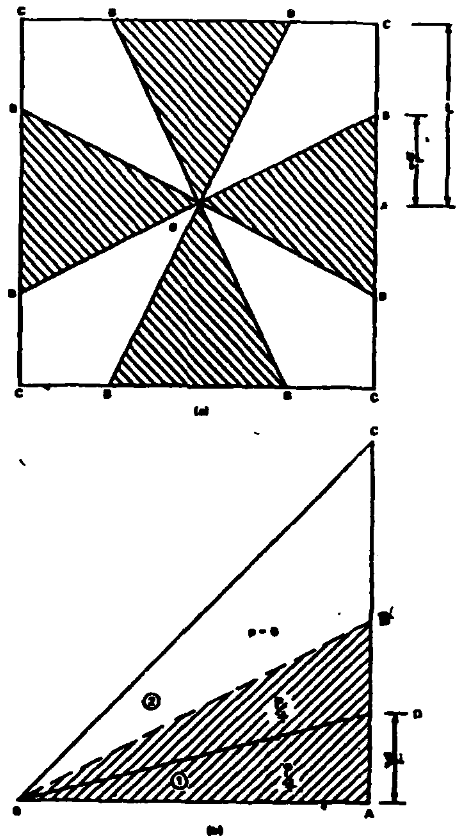

Figure 11: Simply-supported square plate.
(a) Load = p/4 on shaded portion, load = 0 on unshaded portion.
(b) One-eighth of plate for symmetry solution.

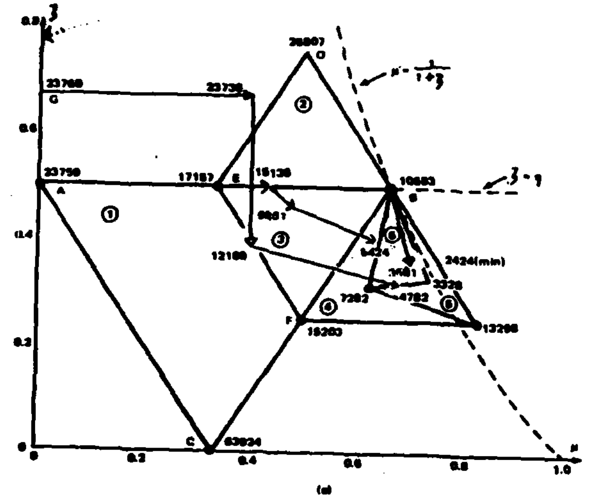

Figure 12a: Location of best upper bound for plate of Figure 11. Arrowed lines show four different gradient search paths. Triangles show simplex solution. Numbers represent 10^5 (p-9.00000).

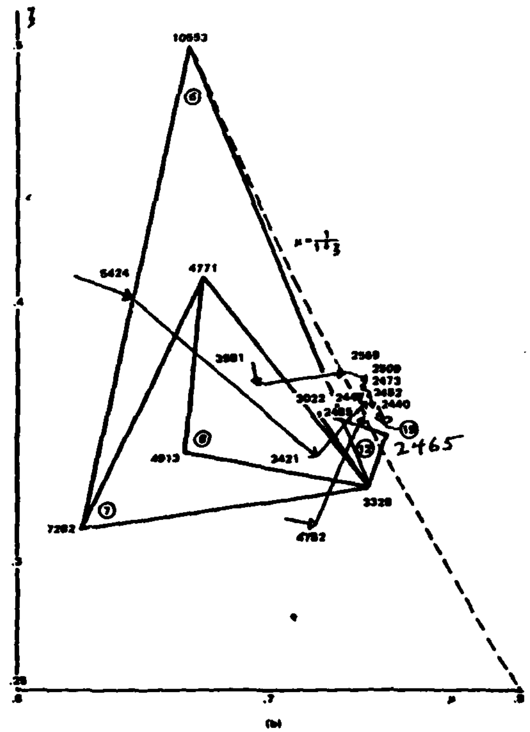

Figure 12(b)

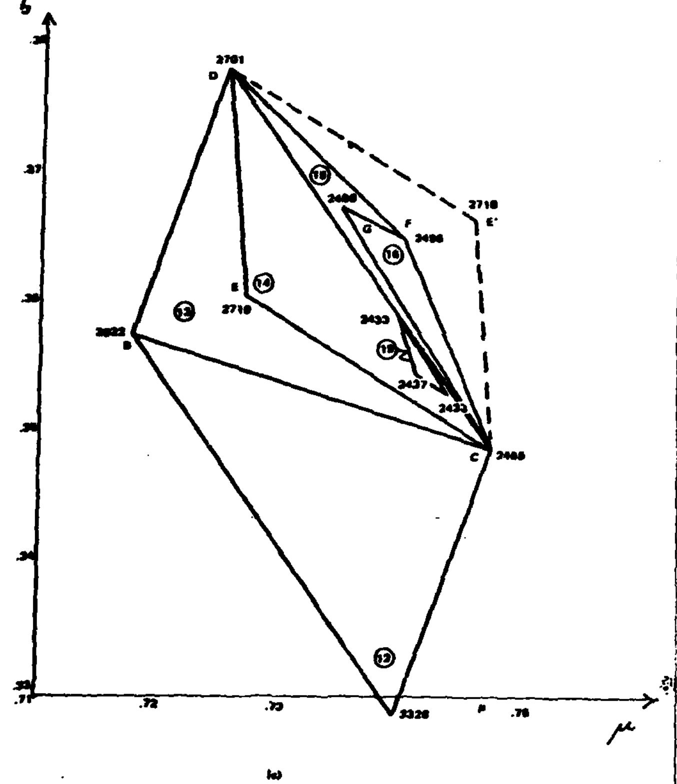

Figure 12(c)

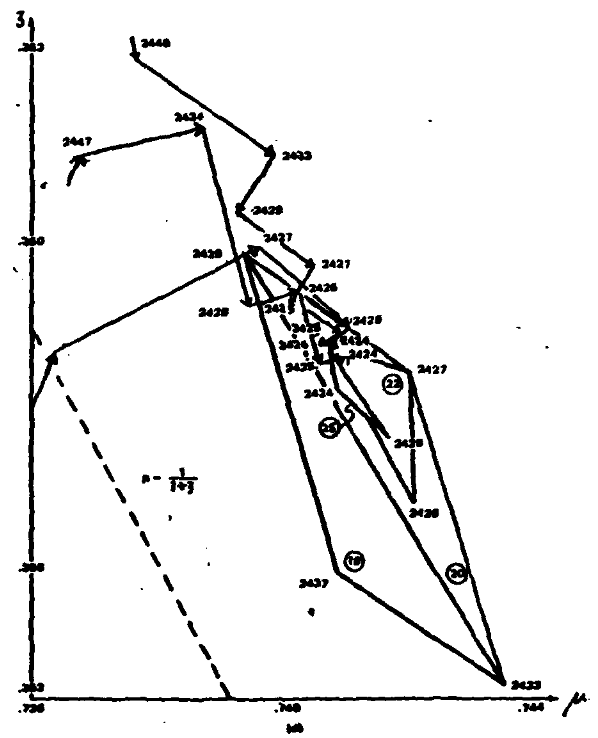

Figure 12(d)

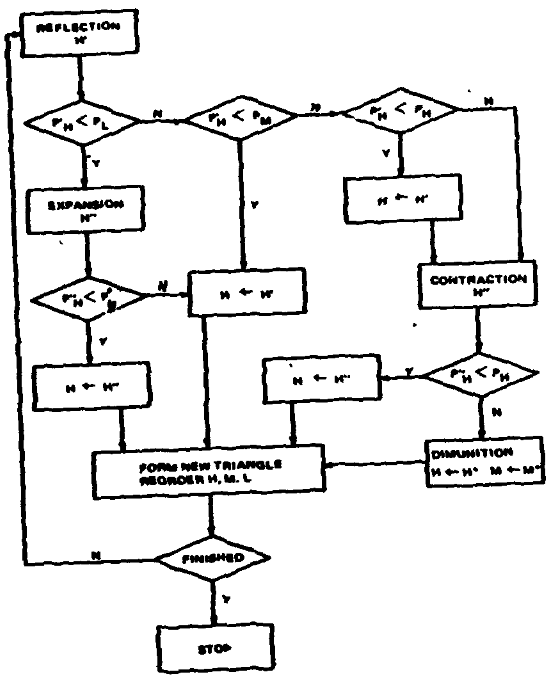

Figure 13: Flow chart for simplex method.

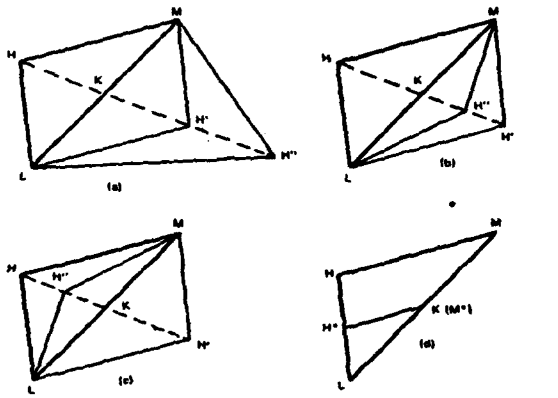

Figure 14: Basic operations for *simplex method*. (a) Reflection H' followed by expansion H". (b) Reflection H' followed by contraction H". (c) Failed reflection H'; contraction H". (d) Dimunition.

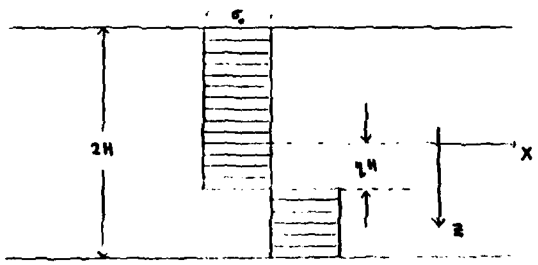

Figure 15: *Fully plastic* stress distribution under combined bending and axial stresses.

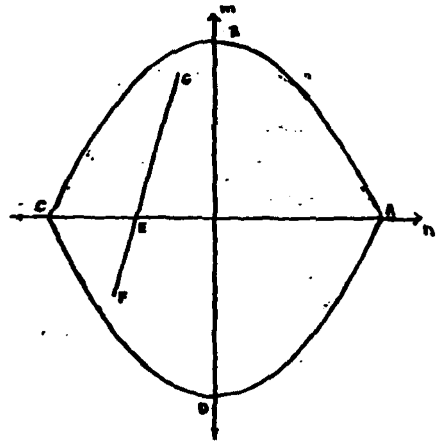

Figure 16: Yield curve and stress profile for a semicircular pinned arch.

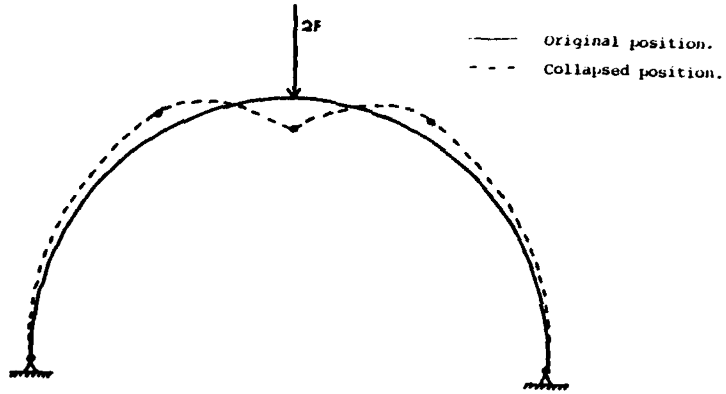

(a)

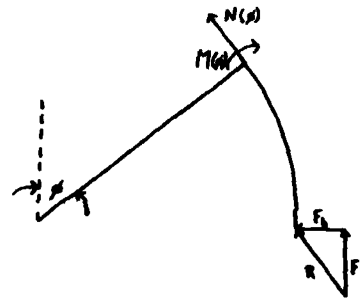

(b)

Figure 17: Semi-circular pinned arch with concentrated load. (a) Collapse mode. (b) Free body diagram.

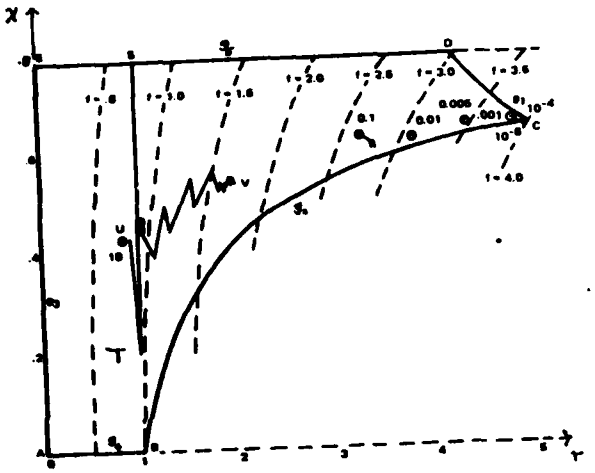

Figure 18: SUMT search for collapse load of pinned arch.

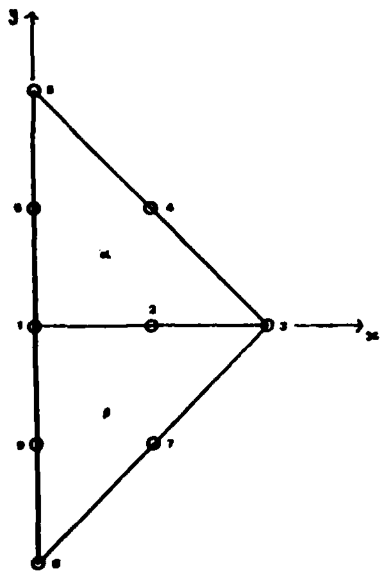

Figure 19: Sample plate elements.

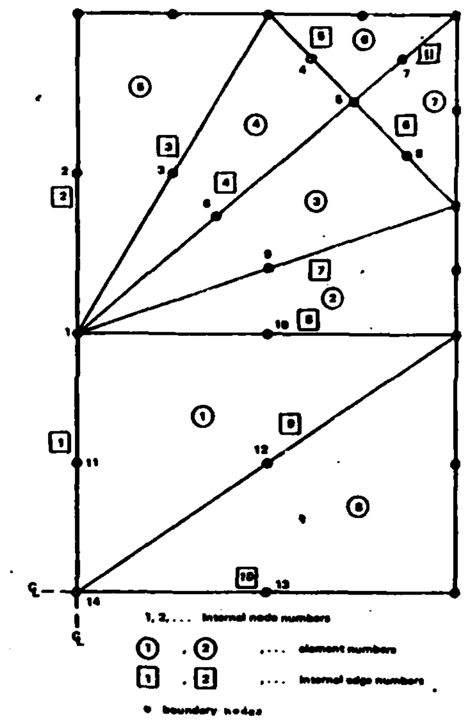

Figure 20: Division of one quadrant of rectangular plate into finite elements [21].

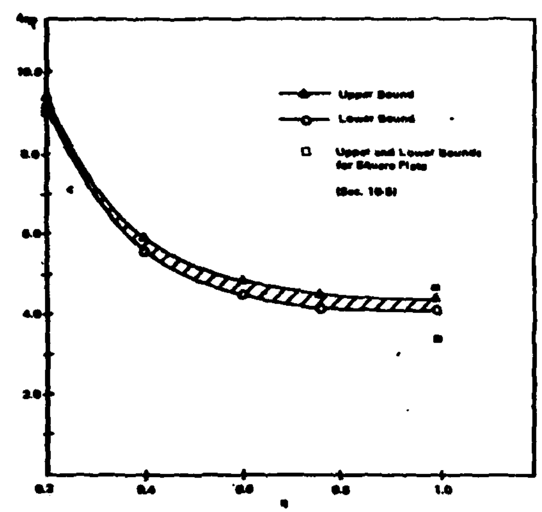

Figure 21: Upper and lower bounds on collapse load of rectangular plates [21]. (η denotes width/length ratio.)

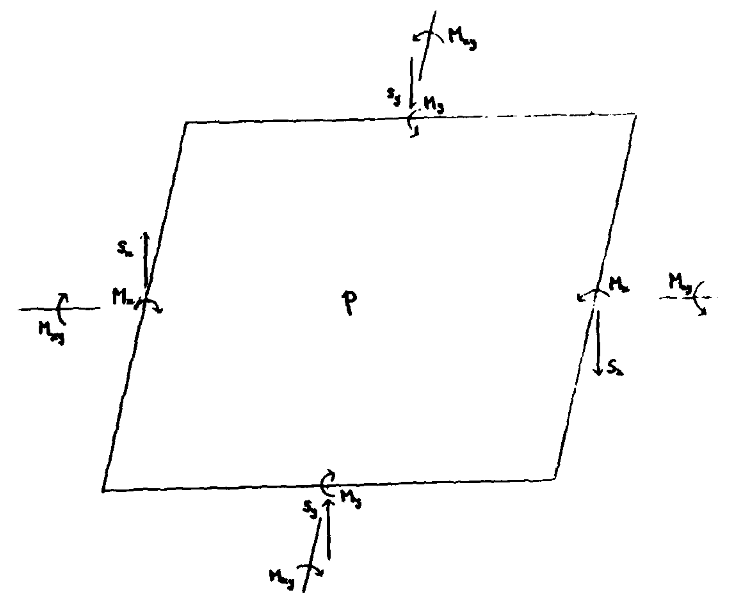

Figure 22: Equilibrium of rectangular plate element.